ERDC/EL TR-08-36

US Army Corps
of Engineers®
Engineer Research and
Development Center

Environmental Quality and Installations Program

UXO Characterization: Comparing Cued Surveying to Standard Detection and Discrimination Approaches

Report 5 of 9
Optimized Data Collection Platforms and Deployment Modes for Unexploded Ordnance Characterization

Stephen D. Billings, Leonard R. Pasion, Kevin Kingdon,
Sean Walker, and Jon Jacobson

September 2008

Environmental Laboratory

Environmental Quality and Installations Program

ERDC/EL TR-08-36
September 2008

UXO Characterization: Comparing Cued Surveying to Standard Detection and Discrimination Approaches

Report 5 of 9
Optimized Data Collection Platforms and Deployment Modes for Unexploded Ordnance Characterization

Stephen D. Billings, Leonard R. Pasion, Kevin Kingdon, Sean Walker, and Jon Jacobson

Sky Research, Inc.
445 Dead Indian Memorial Road
Ashland, OR 97520-9706

Report 5 of 9

Prepared for Headquarters, U.S. Army Corps of Engineers
Washington, DC 20314-1000

Monitored by Environmental Laboratory
U.S. Army Engineer Research and Development Center
3909 Halls Ferry Road, Vicksburg, MS 39180-6199

Abstract: Discrimination and cued-interrogation platforms and procedures developed under contract W912HZ-04-C-0039 are described. Discrimination platform development included: (1) Upgrading Sky's (Sky Research, Inc.) existing EM61 towed array to use five sensors and the Crossbow Inertial Measurement Unit (IMU) for orientation. The IMU significantly improved the positional accuracy of the system. (2) Upgrading a Geonics EM-61 cart-based sensor system to incorporate Robotic Total Station (RTS) positioning, an IMU, and a suspension cart. Compared to a production standard EM-61 positioned with GPS, polarization tensor fits were more accurately positioned and parameter classes more tightly clustered. (3) Upgrading the Geonics EM-63 with RTS, IMU, and a suspension system. Polarization tensor fits were more accurately positioned and parameter classes were more tightly clustered than an equivalent production system. 4) Upgrading a Geometrics G823 magnetometer man-portable quad-sensor array and cart, to include RTS and IMU. Dipole moment depths and locations were more accurate than those predicted from a production level man-portable magnetometer array. Cued-interrogation platforms/procedures development included (1) EM-63 with RTS/IMU/suspension cart and a "magic carpet." Polarization tensor fits to the cued interrogation agreed closely with parameters derived from test stands. (2) GEM-3, 40-cm sensor head and a plywood template. Performance of that system is assessed in Report 9.

Contents

Figures and Tables iv

Preface vi

Unit Conversion Factors vii

Acronyms viii

Executive Summary ix

1 Introduction 1

1.1. Scope of work 1

1.2. Position and orientation system 2

2 EM-61 MK2 Towed Array for Detection and Discrimination 5

2.1. Sensor positioning accuracy tests 8

2.2. System test at the Former Lowry Bombing and Gunnery Range 14

3 EM-61 MK2 Cart for Deployment in a Discrimination Mode 17

4 EM-63 Cart for Deployment in a Discrimination Mode 23

5 Magnetometer Array and Cart for Deployment in a Discrimination Mode 29

6 EM-63 Cart on Cued-Interrogation Mode 33

7 Cued Interrogation with the GEM-3 38

8 Conclusions 40

References 42

Report Documentation Page

Figures and Tables

Figures

Figure 1. Sky Research utilizes the Leica RTS TPS1206 laser positioning system 3
Figure 2. Crossbow AHRS-400 Inertial Measurement Unit. 4
Figure 3. View of the five-element towed array with the RTS prism and crossbow IMU visible. 5
Figure 4. Points measured when defining the geometry of the array. 6
Figure 5. Precision measurements of the geometry of the five-element EM-61 array. 7
Figure 6. Change in the position of the front corner of the array as a function of the roll and pitch angle of the array. 8
Figure 7. RTS survey of the array corners. 9
Figure 8. Two-RTS test of the positional accuracy of the towed array 12
Figure 9. Test of the location accuracy of the towed array system over a 30-second time-period 13
Figure 10. Cumulative distributions of the positional errors for the array when moving. 14
Figure 11. EM-61 MK2, channel 3 test plot data collected at FLBGR 15
Figure 12. Example two-dipole model fit to the first-time channel of the EM-61 towed array. 16
Figure 13. Modified EM-61 discrimination carts developed as part of this project 17
Figure 14. Time channel 3 of EM-61 cart data over the test plot at FLBGR with the locations of buried items shown as black crosses. 18
Figure 15. Recovered polarizations at time channel 1 for the EM-61 with GPS and no IMU and with RTS and IMU 20
Figure 16. Ratio of recovered polarizations at time channels 1 and 4 for the EM-61 with GPS and no IMU and with RTS and IMU 20
Figure 17. Comparison of the predicted versus ground-truth locations for the EM-61 without IMU and with IMU and RTS 21
Figure 18. Comparison of the predicted versus ground-truth depths for the EM-61 without IMU and with IMU and RTS 22
Figure 19. Modified EM-63 cart, which is lower to the ground and has an air suspension system 23
Figure 20. Modified EM-63 cart collecting discrimination mode data at the Ashland test-site. 24
Figure 21. Parameters k_1 and $(k_2 + k_3)/2$ recovered from the EM-63 with GPS and no IMU and with RTS and IMU 25
Figure 22. Pasion-Oldenburg β and γ parameters recovered from the EM-63 with GPS and no IMU and with RTS and IMU 26
Figure 23. Ratio of the primary polarization at time channels 1 and 19 (180 and 10 ms after pulse turn-off) for the EM-63 with GPS and no IMU and with RTS and IMU 26

Figure 24. Comparison of the predicted versus ground-truth locations for the EM-63 without IMU and with IMU and RTS. 27
Figure 25. Comparison of the predicted versus ground-truth depths for the EM-61 without IMU and with IMU and RTS 28
Figure 26. Man-portable quad-sensor array and cart-based magnetometer systems developed as part of this project 29
Figure 27. Scenarios for one- and two-layer measurements 30
Figure 28. Comparison of the predicted versus ground-truth locations for dipole fits to the man-portable array without IMU and the magnetometer cart with IMU 31
Figure 29. Comparison of the predicted versus ground-truth depths for dipole fits to the man-portable array without IMU and the magnetometer cart with IMU 32
Figure 30. Tarpaulin with marked lanes for cued interrogation. 33
Figure 31. Comparison of the predicted versus ground-truth locations for the EM-63 discrimination and cued-interrogation data sets 35
Figure 32. Comparison of the predicted versus ground-truth depths for the EM-63 discrimination and cued-interrogation data sets 36
Figure 33. Parameters k_1 and $(k_2 + k_3)/2$ recovered from the EM-63 deployed in discrimination and cued-interrogation modes 37
Figure 34. Ratio of the primary polarization at time channels 1 and 19 for the EM-63 deployed in discrimination and cued-interrogation modes 37
Figure 35. Schematic of the template used for GEM surveying 38
Figure 36. Template used for GEM-3 Cued Interrogation data collection 39
Figure 37. Schematic of the survey procedure for large targets and multi-object cells using a 1- x 1-m template 39

Tables

Table 1. Various types of equipment developed under this ERDC project. 1
Table 2. Geometry of the towed array in meters relative to the RTS prism. 8
Table 3. Summary of RTS measurements on the corners of the array for four different orientations. 10
Table 4. Comparison of the orientations calculated by the RTS against the orientations measured by the crossbow 10
Table 5. Error in the predicted location of the corners of the array using the uncorrected pitch and roll, compared to a corrected pitch and roll. 11
Table 6. Standard deviations of the location error with and without using the IMU to correct positions. 14

Preface

This report was prepared as part of the Congressional Interest Environmental Quality and Installations Program, Unexploded Ordnance (UXO) Focus Area, Contract No. W912HZ-04-C-0039, Purchase Request No. W81EWF-418-0425, titled, "UXO Characterization: Comparison of Cued Surveying to Standard Detection and Standard Discrimination Approaches." Research was conducted by Sky Research, Inc., for the Environmental Laboratory (EL), U.S. Army Engineer Research and Development Center (ERDC), Vicksburg, MS.

The following Sky Research personnel contributed to this report: Dr. Stephen D. Billings was the project Principal Investigator, oversaw the data collection and analysis of the field data, and produced the report for this segment of the project; Dr. Leonard Pasion conducted quality control of the parametric inversions; Kevin Kingdon, Jon Jacobson, and Sean Walker assisted with the platform developments, data collection, and processing of the data; and Joy Rogalla was the copy editor for this report.

This project was performed under the general supervision of Dr. M. John Cullinane, Jr., Technical Director, Military Environmental Engineering and Sciences, EL; and John H. Ballard, Office of Technical Director and UXO Focus Area Manager, EL. Reviews were provided by Mr. Ballard and Dr. Dwain Butler, Alion Science and Technology Corporation. Dr. Beth Fleming was Director, EL.

COL Gary E. Johnston was Commander and Executive Director of ERDC. Dr. James R. Houston was Director.

Unit Conversion Factors

Multiply	By	To Obtain
acres	4,046.873	square meters
degrees (angle)	0.01745329	radians
inches	0.0254	meters

Acronyms

cm	centimeter(s)
DAS	Data Acquisition System
DMU	Data Management Units
DoD	Department of Defense
DSB	Defense Science Board
EM	Electromagnetic
EMI	Electromagnetic Induction
ERDC	Engineer Research and Development Center
FLBGR	Former Lowry Bombing and Gunnery Range
GPR	Ground Penetrating Radar
GPS	Global Positioning System
IMU	Inertial Measurement Unit
m	meter(s)
RTK GPS	Real-time Kinematic Global Positioning System
RTS	Robotic Total Station
UXO	Unexploded Ordnance

Executive Summary

The clearance of military facilities in the United States contaminated with unexploded ordnance (UXO) is one of the most significant environmental concerns facing the Department of Defense (DoD). A 2003 report by the Defense Science Board (DSB) on the topic estimated costs of remediation as tens of billions of dollars. The DSB recognized that development of effective discrimination strategies to distinguish UXO from non-hazardous material is one essential technology area where the greatest cost saving to the DoD can be achieved.

The objective of project W912HZ-04-C-0039 "UXO Characterization: Comparison of Cued Surveying to Standard Detection and Standard Discrimination Approaches" was to research, develop, optimize, and evaluate the efficiencies of various modes of UXO characterization and remediation as a function of the density of UXO and associated clutter. Survey modes investigated in the research include:

1. Standard detection survey: All selected anomalies are excavated;
2. Advanced discrimination survey: Data collected in proximity to each identified anomaly are inverted for physics-based parameters and statistical or analytical classifiers are used to rank anomalies, from which a portion of the higher ranked anomalies are excavated;
3. Cued survey mode: Each selected anomaly is revisited with an interrogation platform, high-quality data are collected and analyzed, and a decision is made as to whether to excavate the item, or leave it in the ground.

Specific technical objectives of the research were to:

- Determine the feasibility and effectiveness of various interrogation approaches based on the cued-survey approach;
- Determine the feasibility and effectiveness of various interrogation sensors including magnetics, ground penetrating radar (GPR), and electromagnetic (EM) induction (EMI), and evaluate combinations of these sensors;
- Develop and evaluate the most promising interrogation platform designs;

- Develop optimal processing and inversion approaches for cued-interrogation platform data sets;
- Evaluate the data requirements to execute accurate target parameterization and assess the technical issues of meeting these requirements using detection and interrogation survey techniques;
- Determine which survey mode is most effective as a function of geological interference, and UXO/clutter density;
- Investigate the feasibility and effectiveness of using detailed test-stand measurements on UXO and clutter to assist in the design of interrogation algorithms used in the cued-search mode.

The main areas of research involved in these coordinated activities include:

- Sensor phenomenology including GPR, EMI, and magnetometry;
- Data collection systems; platforms, field survey systems, field interrogation systems;
- Parameter estimation techniques; inversion techniques (single, cooperative, joint), forward-model parameterizations, processing strategies;
- Classification methods; thresholding, statistical models, information systems.

This report "UXO Characterization: Comparing Cued Surveying to Standard Detection and Discrimination Approaches: Report 5 of 9 – Optimized Data Collection Platforms and Deployment Modes for Unexploded Ordnance Characterization" is one of a series of nine reports written as part of W912HZ-04-C-0039:

1. UXO Characterization: Comparing Cued Surveying to Standard Detection and Discrimination Approaches: Report 1 of 9 – Summary Report;
2. UXO Characterization: Comparing Cued Surveying to Standard Detection and Discrimination Approaches: Report 2 of 9 – Ground Penetrating Radar for Unexploded Ordnance Characterization; Fundamentals;
3. UXO Characterization: Comparing Cued Surveying to Standard Detection and Discrimination Approaches: Report 3 of 9 – Test Stand Magnetic and Electromagnetic Measurements of Unexploded Ordnance;

4. UXO Characterization: Comparing Cued Surveying to Standard Detection and Discrimination Approaches: Report 4 of 9 – UXO Characterization Using Magnetic, Electromagnetic, and Ground Penetrating Radar Measurements at the Sky Research Test Plot;
5. UXO Characterization: Comparing Cued Surveying to Standard Detection and Discrimination Approaches: Report 5 of 9 – Optimized Data Collection Platforms and Deployment Modes for Unexploded Ordnance Characterization;
6. UXO Characterization: Comparing Cued Surveying to Standard Detection and Discrimination Approaches: Report 6 of 9 – Advanced Electromagnetic and Magnetic Methods for Discrimination of Unexploded Ordnance;
7. UXO Characterization: Comparing Cued Surveying to Standard Detection and Discrimination Approaches: Report 7 of 9 – Marine Corps Base Camp Lejeune: UXO Characterization Using Ground Penetrating Radar;
8. UXO Characterization: Comparing Cued Surveying to Standard Detection and Discrimination Approaches: Report 8 of 9 – Marine Corps Base Camp Lejeune: UXO Characterization Using Magnetic and Electromagnetic Data;
9. UXO Characterization: Comparing Cued Surveying to Standard Detection and Discrimination Approaches: Report 9 of 9 – Former Lowry Bombing and Gunnery Range: Comparison of UXO Characterization Performance Using Area and Cued-interrogation Survey Modes.

1 Introduction

A significant component of the work conducted under this contract involved the modification and development of discrimination and cued-interrogation platforms and procedures. This report describes these modifications and in each case compares the performance of the modified system to a baseline system (Table 1). Typically this comparison was conducted using data collected at either the Ashland test plot or the Former Lowry Bombing and Gunnery Range (FLBGR) geophysical prove-out grid. Deployment of the modified systems to either Camp Lejeune or the Rocket Range and 20-mm Range Fan sites on FLBGR are described in those reports (Table 1).

Table 1. Various types of equipment developed under this ERDC project.

Type	Category	Comparison	Ashland Test Plot	FLBGR			Camp Lejeune
				GPO	RR	20 mm	
EM-61 towed array with RTS, IMU	Discrimination	Itself (no IMU)	x	x	x	x	x
EM-61 cart with IMU, RTS, suspension	Discrimination	EM-61 GPS	x				
Magnetometer array with RTS/IMU	Discrimination	Magnetometer array without IMU	x	x	x	x	x
Magnetometer cart with RTS/IMU	Discrimination	Magnetometer array with RTS/IMU	x				
EM-63 with IMU/RTS/Suspension	Discrimination	EM-63 with GPS	x	x	x	x	x
EM-63 with IMU/RTS/ Suspension/Magic Carpet	Cued interrogation	EM-63 discrimination	x	x	x	x	x
GEM-3 template	Cued interrogation	Other EM instruments	x	x	x	x	

1.1. Scope of work

The following discrimination mode platforms were modified or developed:

1. Sky Research's existing three-element EM-61 towed array was upgraded to a five-element towed array with a Crossbow Inertial Measurement Unit (IMU) used for sensor orientation and refinement of array positioning. This system was used to collect data at all sites;

2. Modifications to the Geonics EM-61 cart-based sensor systems to incorporate an RTS positioning and a crossbow IMU for orientation, as well as a suspension system. This system was used on the Ashland test plot as well as for preliminary surveys at FLBGR;
3. Geonics EM-63 suspension cart with RTS positioning and Crossbow IMU for orientation. This system was deployed to all sites;
4. Geometrics G823 magnetometer man-portable quad-sensor array and man-portable cart, both with RTS positioning and Crossbow IMU for orientation. One of these systems was deployed at each site.

The original intent was to deploy the 96-centimeter (cm) head GEM-3 sensor in a discrimination mode. However, reliable data could never be extracted from this instrument and it was therefore eliminated from consideration.

In addition to the modifications to discrimination mode systems described above, the following cued-interrogation platforms/procedures were developed:

1. EM-63 cued-interrogation procedure based on the suspension cart and a "magic carpet" comprising a 2.5-meter (m) by 2.5-m tarpaulin with lanes pre-marked at 25-cm spacing. This system was used to collect data at all sites;
2. GEM-3 cued-interrogation procedure based on 40-cm sensor head and a 1-m by 1-m plywood template. Data were collected on the Ashland test plot and at FLBGR.

1.2. Position and orientation system

The Leica TPS 1206 RTS and the Crossbow AHRS 400 IMU were key components of each of the systems developed as part of this project.

In 2005, Leica introduced the TPS1200 series as the most advanced RTS system commercially available. The Leica RTS system (Figure 1) provides three-dimensional (3-D) position solutions at a rate of up to 8 Hz with sub-centimeter accuracy. The system operates as a high-precision total station and defines the position of a 360-degree prism to a distance of approximately 1,000 m. The robotic component of the system is the ability of the RTS to track the prism while it is moving. Operationally, the total station is located over a known point in proximity of the survey area, and a second point is utilized to establish a survey baseline. Once established,

the RTS can track the prism while it is deployed on the geophysical survey platform.

Figure 1. Sky Research utilizes the Leica RTS TPS1206 laser positioning system. This device is set up over a known point and tracks a prism attached to the geophysical survey equipment. RTS technology out-performs GPS in terms of accuracy, sampling rate, and operational ease of use.

The Crossbow AHRS-400 IMU was used for measuring the pitch, roll, and yaw of each sensor system (Figure 2). The AHRS series units are low power, fast turn on, reliable, and provide accurate solutions for geophysical survey applications. The AHRS-400 series of products utilize a sophisticated Kalman filter algorithm to allow the unit to track orientation accurately through dynamic maneuvers and automatically adjust for changing dynamic conditions without any external user input. The AHRS is the solid-state equivalent of a vertical gyro/artificial horizon display combined with a directional gyro. The AHRS is a nine-axis measurement system that combines linear accelerometers, rotational rate sensors, and magnetometers. The AHRS uses the three-axis accelerometer and three-axis rate sensor to make a complete measurement of the dynamics of the system. The addition of a three-axis magnetometer also allows the AHRS to make a true measurement of magnetic heading. For the EM systems, the crossbow is typically placed within approximately 0.5 m of the transmitter coils and the heading output is unreliable. Consequently, successive GPS measurements are used to estimate the azimuth (yaw) of those systems.

Figure 2. Crossbow AHRS-400 Inertial Measurement Unit.

Crossbow Technology Data Management Units (DMUs) employ onboard digital processing to compensate for deterministic error sources within the unit and to compute attitude information. The DMUs accomplish these tasks with an analog-to-digital converter and a high-performance Digital Signal Processor.

2 EM-61 MK2 Towed Array for Detection and Discrimination

In 2005, Sky Research used a three-coil EM-61 MK2 towed array for two field seasons at FLBGR. As part of this project, the array was modified to include two additional EM-61 sensors as well as the Crossbow AHRS-400 IMU. The data acquisition system (DAS) was also modified to accommodate the increased number of sensors. Coils were deployed in a 5×1 arrangement, with the long axis of the 1-m by 0.5-m EM-61 coils oriented in the direction of travel (Figure 3).

Figure 3. View of the five-element towed array with the RTS prism and crossbow IMU visible.

The crossbow was mounted as close to the center of the middle coil as possible. The crossbow could not be mounted directly on the floor of the array, as the crossbow has an aluminum box that would create a noise signal. In addition, the primary field from the transmitter overwhelms the crossbow electronics, resulting in the output of inaccurate pitch and roll angles. The unit was first mounted on the RTS prism pole, directly under the RTS prism. However, the unit stopped working after suffering large impulsive shocks when traversing over rough ground. The unit was then moved to the horizontal fiberglass bar that connects the array to the tow vehicle. It was placed directly over the middle of the center coil about 60 cm above the array bottom. This location was found to be ideal as the toe-bar is rigidly connected to the array and tracks the array orientation very closely. In addition, the crossbow was low enough to reduce the size of the impulsive shocks experienced by the unit when traversing over rough ground. At this location, the magnetic heading readings output by the unit were not reliable. By tracking the position of the RTS, the azimuth of the unit can be estimated to a reasonable level of accuracy.

Positioning each sensor requires the 3-D location of the RTS prism, the orientation information provided by the crossbow, and a precise measure of the position of each sensor relative to the RTS prism. A 3-ft Arc Second Total Station instrument with a precision miniature prism was used to accurately determine the array geometry (Figures 4 and 5). Each of the locations marked in Figure 4 were surveyed with the Seco precision prism with a horizontal and vertical accuracy of ±6 mm. The locations of the centers of each coil and the crossbow IMU relative to the RTS prism are given in Table 2.

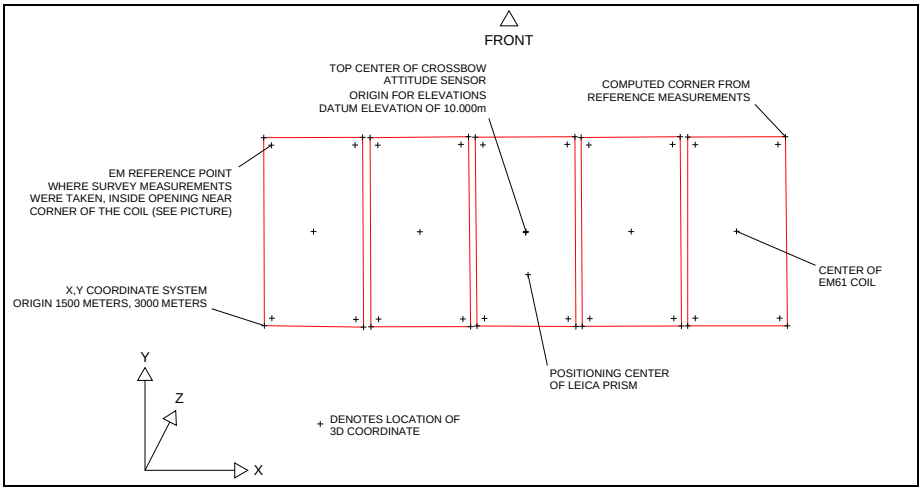

Figure 4. Points measured when defining the geometry of the array.





Top left: Miniature prism on EM reference point.

Top right: EM reference point at top center of the larger opening.

Center left: Measuring the location of the IMU.

Center right: Seco miniature prism with bubble level.

Bottom left: Sokkia 3 arc second SET Total Station.

Figure 5. Precision measurements of the geometry of the five-element EM-61 array.

Table 2. Geometry of the towed array in meters relative to the RTS prism.

Location	Sideways Offset	Forward Offset	Vertical Offset
Far left coil	-1.097	0.215	-1.245
Middle left coil	-0.555	0.216	-1.246
Center coil	-0.016	0.217	-1.241
Middle right coil	0.522	0.217	-1.244
Far-right coil	1.062	0.217	-1.241
Top center crossbow	-0.014	0.212	-0.540

2.1. Sensor positioning accuracy tests

The accuracy of the crossbow orientations and the accuracy with which the positions of the four corners of the array could be predicted were evaluated next. The array corners have the longest lever arms relative to the RTS prism location and will therefore experience the greatest positional change as the pitch and roll of the array changes. The top-left and top-right corners have the longest lever arms (135 cm laterally, 70 cm forwards, and 125 cm below the location of the RTS prism). Figure 6 shows the extent of the movement of one of the front corners as a function of pitch and roll. Total movement translates to about 2.5 cm for every degree of roll and 3.2 cm for every degree of pitch. Thus, even 4 degrees of roll or pitch translates to a 10-cm or greater error in the location of the array corner.

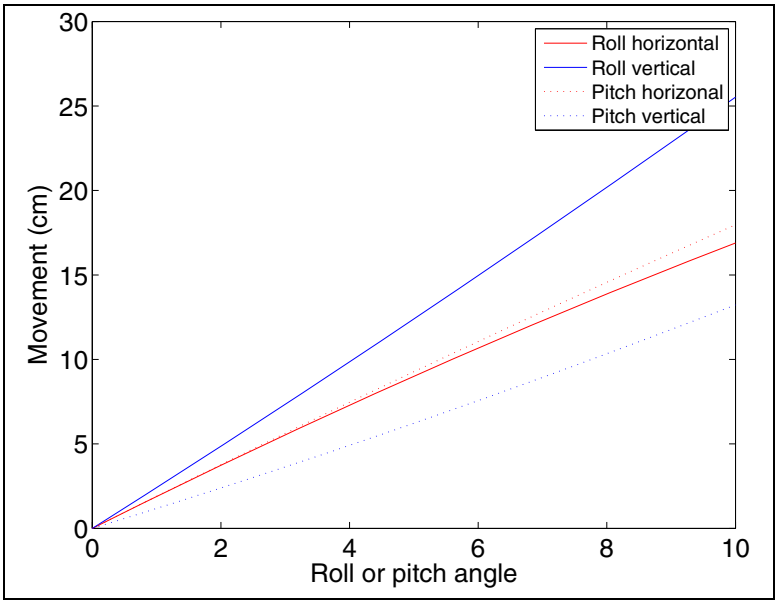

Figure 6. Change in the position of the front corner of the array as a function of the roll and pitch angle of the array.

Figure 7. RTS survey of the array corners.

The first test of the accuracy of the RTS/Crossbow system was static. The four corners of the array were accurately measured with the RTS (Figure 7) while flat, then rolled[1] by approximately 5 degrees, then pitched[2] by 10 degrees and finally, pitched and rolled by about 10 degrees each. Immediately after each of these measurements, the RTS prism was returned to its usual position on the array, and 15 seconds of RTS positions and crossbow orientations were logged on the DAS. RTS positions of the corners and of the prism are given in Table 3. In each case, the rear-left corner is assumed to be the origin of the coordinate system. The x, y, and z directions are relative to a geographic reference (not relative to the array). A best-fitting plane was fit to the measurements of the four corners of the array (the differences between the position of the best-fitting plane and the four points are listed in the last column of Table 3). Pitch and roll angles were calculated and compared to the pitch and roll angles recorded by the crossbow (Table 4).

The values are in close agreement (generally <0.1 degree), which demonstrates that the coordinate system of the crossbow is closely aligned with the coordinate system of the array. Using the raw crossbow values, the positions of the corner of the array would be in error by the amounts shown in Table 5. Thus, at least in a static mode, the array can be positioned with an accuracy of less than 1 cm, and in many cases less than 0.3 cm.

The results described in the last paragraph demonstrate that very little error is introduced by assuming the crossbow and towed array are perfectly aligned. A procedure was developed, however, to correct for the orientation difference between the crossbow and array. This involves taking at least two static measurements as described above. Applying this correction procedure to the four orientations in Table 3 indicates that the Crossbow coordinate system was at a roll of -0.03 degree, pitch of 0.18 degree, and an azimuth (or yaw) of -0.89 degree relative to the array coordinate system. Adjusting the crossbow orientations using this information, the corners of the array can be predicted to an accuracy of generally better than 0.1 cm.

[1] Roll is defined as the sidewards orientation of the array, with a roll to the right positive.

[2] Pitch is defined as roll forwards/backwards, with a forwards pitch positive.

Table 3. Summary of RTS measurements on the corners of the array for four different orientations.

Location	Easting, cm	Northing, cm	Elevation, cm	Plane Error, cm
Flat				
Front-left	0.33	0.82	-0.01	0.05
Rear-Left	0.00	0.00	0.00	-0.05
Rear-Right	2.41	-0.92	0.06	0.05
Front-Right	2.75	-0.10	0.05	-0.05
RTS-prism	1.29	-0.25	1.30	NA
Roll				
Front-left	0.29	0.83	-0.04	-0.41
Rear-Left	0.00	0.00	0.00	0.41
Rear-Right	2.41	-0.84	-0.44	-0.41
Front-Right	2.69	0.00	-0.46	0.41
RTS-prism	1.50	-0.25	1.02	NA
Pitch				
Front-left	0.30	0.82	-0.17	-0.02
Rear-Left	0.00	0.00	0.00	0.02
Rear-Right	2.44	-0.86	0.06	-0.02
Front-Right	2.73	-0.06	-0.11	0.02
RTS-prism	1.37	-0.01	1.24	NA
Roll and pitch				
Front-left	0.28	0.83	-0.14	-0.10
Rear-Left	0.00	0.00	0.00	0.10
Rear-Right	2.41	-0.90	-0.20	0.10
Front-Right	2.71	-0.08	-0.34	-0.10
RTS-prism	1.45	-0.10	1.12	NA

Table 4. Comparison of the orientations calculated by the RTS to the orientations measured by the crossbow.

Orientation	Roll (degrees)			Pitch (degrees)		
	Plane	IMU	Diff	Plane	IMU	Diff
Flat	-1.29	-1.07	-0.22	-0.73	-0.89	0.17
Roll	4.44	4.63	-0.19	-1.93	-2.04	0.11
Pitch	-1.29	-1.29	0.01	-10.97	-11.21	0.25
Roll and Pitch	9.70	9.77	-0.07	-9.18	-9.20	0.02

Table 5. Error in the predicted location of the corners of the array using the uncorrected pitch and roll, compared to a corrected pitch and roll.

Location	Uncorrected			Corrected		
	Sideways cm	Forwards cm	Elevation cm	Sideways cm	Forwards cm	Elevation cm
Flat						
Front-left	-0.19	-0.14	0.07	-0.07	-0.13	-0.05
Rear-Left	-0.18	-0.13	0.24	-0.07	-0.12	0.07
Rear-Right	-0.27	-0.20	-0.08	-0.10	-0.18	0.01
Front-Right	-0.27	-0.21	-0.25	-0.10	-0.18	-0.11
Roll						
Front-left	-0.64	-0.31	0.31	-0.07	-0.09	0.01
Rear-Left	-0.62	-0.24	0.68	-0.07	-0.07	0.08
Rear-Right	-0.65	-0.41	-0.29	-0.07	-0.08	0
RTS-prism	-0.68	-0.47	-0.66	-0.07	-0.1	-0.07
Pitch						
Front-left	-0.36	0.15	0.45	0.03	0.2	0.12
Rear-Left	-0.36	0.16	0.48	0.02	0.18	-0.01
Rear-Right	-0.47	0.04	-0.37	0.02	0.2	-0.1
Front-Right	-0.47	0.04	-0.41	0.03	0.22	0.03
Roll and pitch						
Front-left	-0.12	-0.36	-0.21	0.13	0.04	-0.07
Rear-Left	-0.11	-0.36	0.05	0.13	0.04	-0.12
Rear-Right	-0.11	-0.34	0.09	0.13	0.04	0.1
Front-Right	-0.11	-0.34	-0.17	0.13	0.04	0.15
Average						
All points	0.35	0.24	0.30	0.08	0.12	0.07

The results described above were collected while the array was stationary. The next goal was to determine how the positional accuracy increased when the system was moving. During April 2006, two RTS units were set up at the Ashland test plot and a second prism was placed on the rear-right corner of the array (Figure 8). One base station tracked the main prism, while the other tracked the second prism on the bottom corner of the array. IMU and RTS outputs of both systems were then streamed into the DAS. Merging the two RTS streams using the time base as a reference led to an approximate determination of the accuracy of the RTS/IMU corrected positions of the array. As the second prism was located on the front corner of the array, it has the longest possible lever arm relative to the RTS, and hence will move the most as the system pitches and rolls.

The second prism was 137.4 cm to the left, 66.6 cm forwards, and 109.3 cm below the main prism. Note that the error in position estimated using this method will be approximate, as the position of the reference prism can only be determined to within approximately 1 cm (at best).

Figure 8. Two-RTS test of the positional accuracy of the towed array. Rectangular pieces of card-board were used to shield each prism from the other RTS base-station. At the end of each line, the card-board was moved to the other side of the each prism so that the same gun tracked the same prism.

A 30-second section of data collected north-south that displayed about a 5-degree change in both pitch and roll was used to calculate the error in position (Figure 9a). The RTS base stations were located approximately perpendicular to the direction of travel, and the northing value changed much more rapidly than easting or elevation (Figure 9b). During each RTS measurement, the cart moved about 20 cm. Actual and predicted positions of the second prism were compared (Figures 9c, 9d, 9e, and 9f, 10, and Table 6), both with and without IMU corrections. Using the IMU, 90 percent of predicted locations are within 8 cm of the measured location with a maximum error of 30 cm. Most of the error is in the northing with a standard deviation of 7.1 cm: the easting and elevation measurements have standard deviations of 1.1 and 0.73 cm, respectively. The northing has a larger error because it is the coordinate that is changing the fastest. There are two potential sources for this error:

1. Inaccurate time-stamping of RTS locations within the DAS, which is a Windows-based application. As such, events can typically only be time-stamped to within an accuracy of about 20 ms. During data collection, the array was moving at approximately 100 cm every second, so that a 20-ms error in timing will translate to a 2-cm error in position. The DAS times are used for both prisms; therefore, this location error will be effectively doubled.
2. Inaccurate tracking of the prism by the RTS base station. Inspection of Figure 9b (which shows the change in RTS position between successive measurements) reveals a number of occasions where the northing value changes by a large amount, followed by a much smaller change (or vice

versa). These events are not always correlated with events in the IMU. An example of this is the event in the northing plot at 28 seconds in Figure 9b where two values are almost 60 cm apart and the next two are almost 0 cm apart. Here, it appears that the RTS tracking algorithm has overshot the true position and then waited for the prism to "catch up."

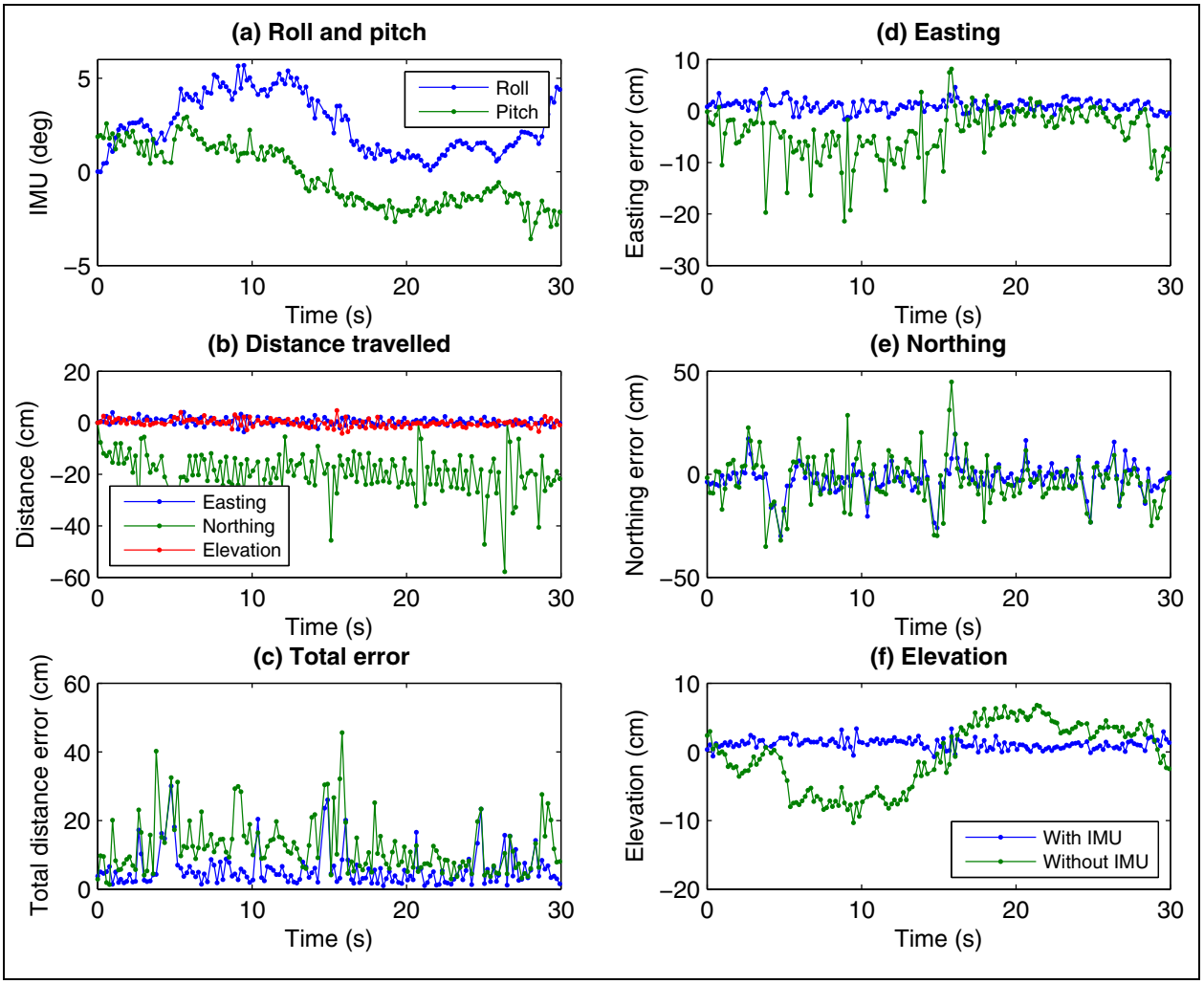

Figure 9. Test of location accuracy of the towed array system over a 30-second time period: (a) Variation in pitch and roll; (b) Distance moved between each RTS measurement; (c) Total error with and without IMU corrections; and (d) to (f) errors in the prediction of the easting, northing, and elevation of the second prism.

The corners of the array can be predicted with greater accuracy when using the IMU (Figures 9 and 10, and Table 6). The improvement is most significant for the easting and northing, where there is at least a fourfold reduction in the standard deviation.

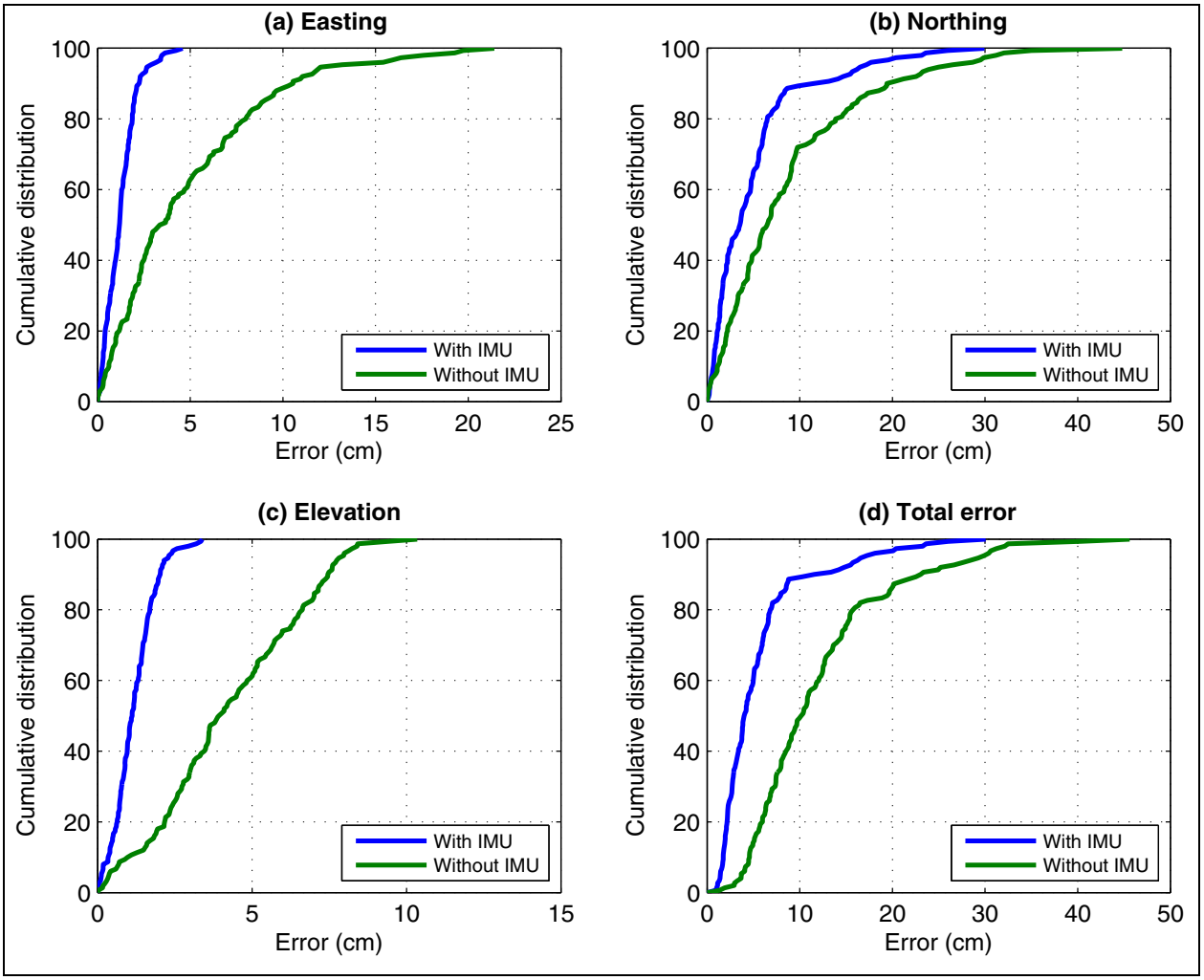

Figure 10. Cumulative distributions of the positional errors for the array when moving.

Table 6. Standard deviations of the location error with and without using the IMU to correct positions.

Component	Easting, cm	Northing, cm	Elevation, cm
With IMU	1.1	7.1	0.73
Without IMU	4.9	11.7	4.8

2.2. System test at the Former Lowry Bombing and Gunnery Range

In a shakedown test of the five-element towed array system on the test grid at FLBGR, 120 of 123 buried items were successfully detected using a 3-mV threshold on the third time channel (Figure 11).

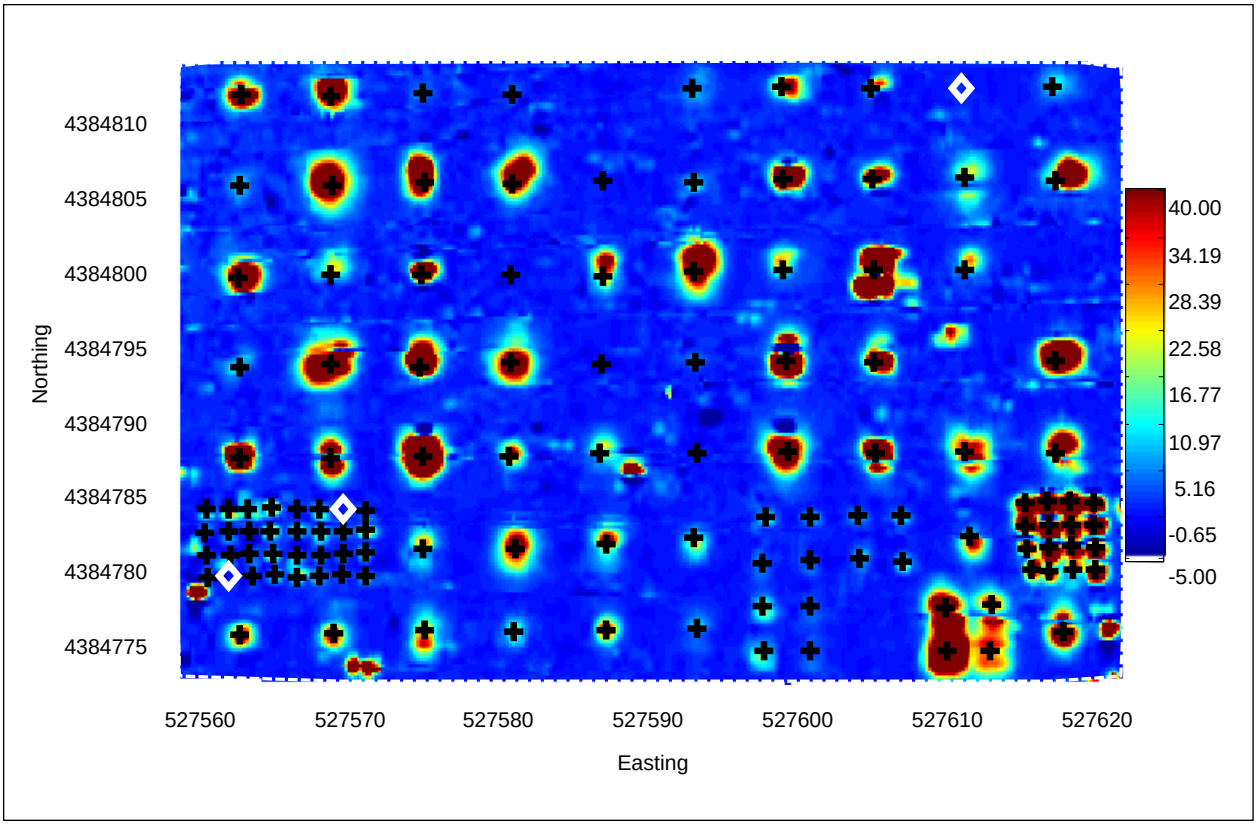

Figure 11. EM-61 MKII, channel 3 test plot data collected at FLBGR. Targets detected assuming a threshold of 3 mV on channel 3 are shown as black crosses. Three undetected targets are shown as white diamonds.

Detected items included many small fuzes and 20-mm projectiles down to the 30-cm depth, and a number of larger objects at depths down to 1.2 m. The three undetected items included a small fuse at 8 cm, a 20-mm projectile at 30 cm, and an M38 at 60 cm.

Note that the negative transients and stripes in the data are not indicative of a problem. They occur because the system acts as one large transmitter with five receivers, with each coil close to the ground. If the same object was measured under each coil, the two outer coils would respond differently than the two inner coils, which in turn would have a different response to the central coil. The negative transients generally occur in the two outer coils and arise due to the primary field lying in a more horizontal direction than it does beneath the three central coils. The secondary field is directed downwards through the coil (instead of upwards), which causes the voltage to go negative. To demonstrate that the negative transients are a natural consequence of the coil geometry, the data were fit over one of the anomalies with a two-dipole model (Figure12). The negative transients are reproduced well by the model recovered by inversion.

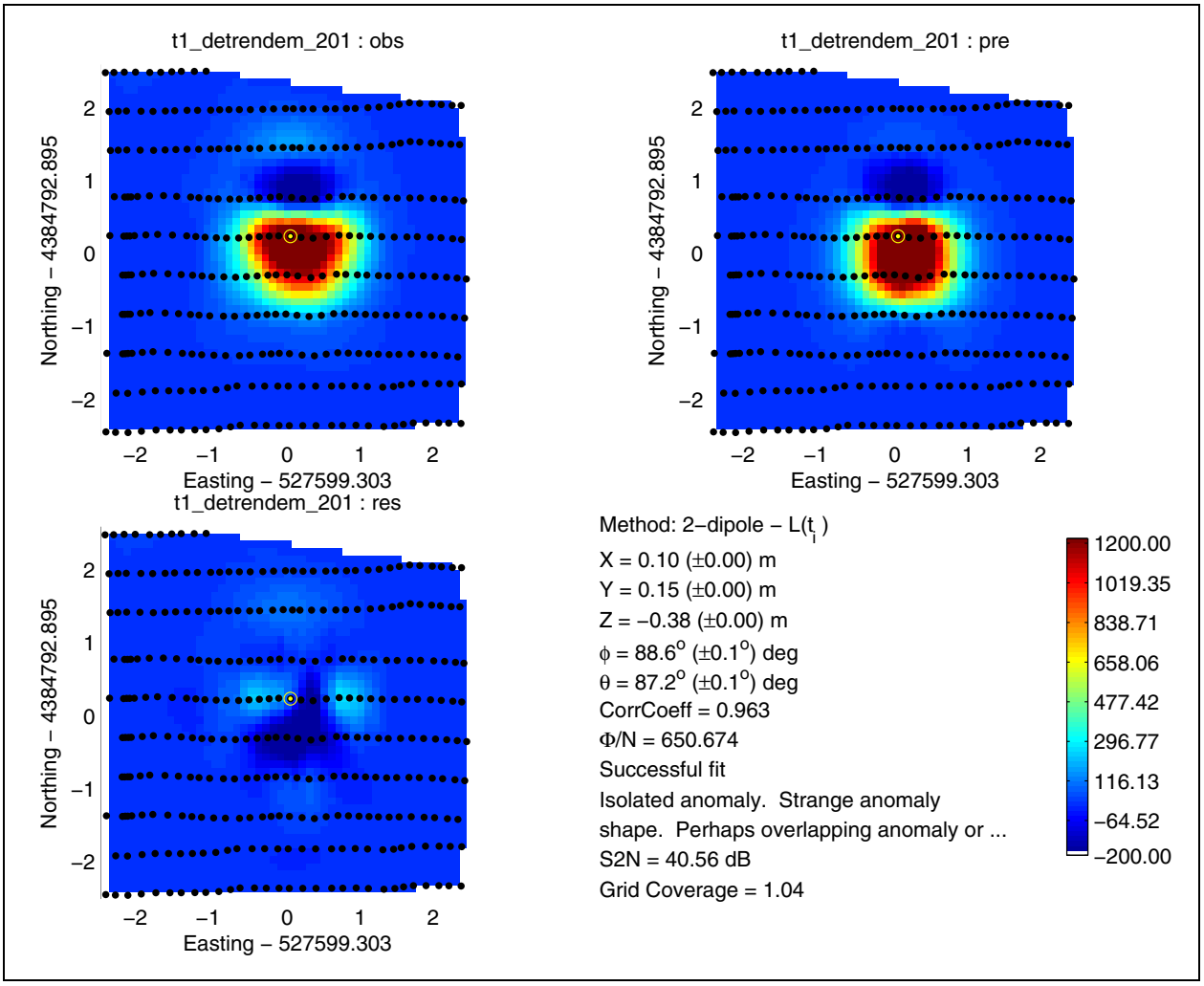

Figure 12. Example two-dipole model fit to the first-time channel of the EM-61 towed array. Notice the large negative feature on the outer coil, which is reproduced well by the model recovered by inversion.

The use of RTS and an IMU have significantly improved the positional and orientation accuracy of the towed-array system. The location accuracy of the system is fundamentally limited by the timing resolution of a Windows-based DAS, and the capability of the RTS to continuously track the prism. The furthest corner of the array can generally be positioned to within 5–8 cm, with occasional inaccurate readings that will be in error by up to 30 cm.

3 EM-61 MK2 Cart for Deployment in a Discrimination Mode

Improvements to the EM-61 discrimination cart were conducted in two stages:

1. The Crossbow IMU was installed directly below the RTS prism on a pole above the center of the EM-61 transmitter (Figure 13a). These modifications were completed in 2005 and the system was used to collect data at the FLBGR test grid and at the Rocket Range and 20-mm Range Fan;
2. In early 2006, the coils were placed on a suspension cart and the crossbow was relocated closer to the center of gravity (Figure 13b). This modified system was used to collect data on the Ashland test plot.

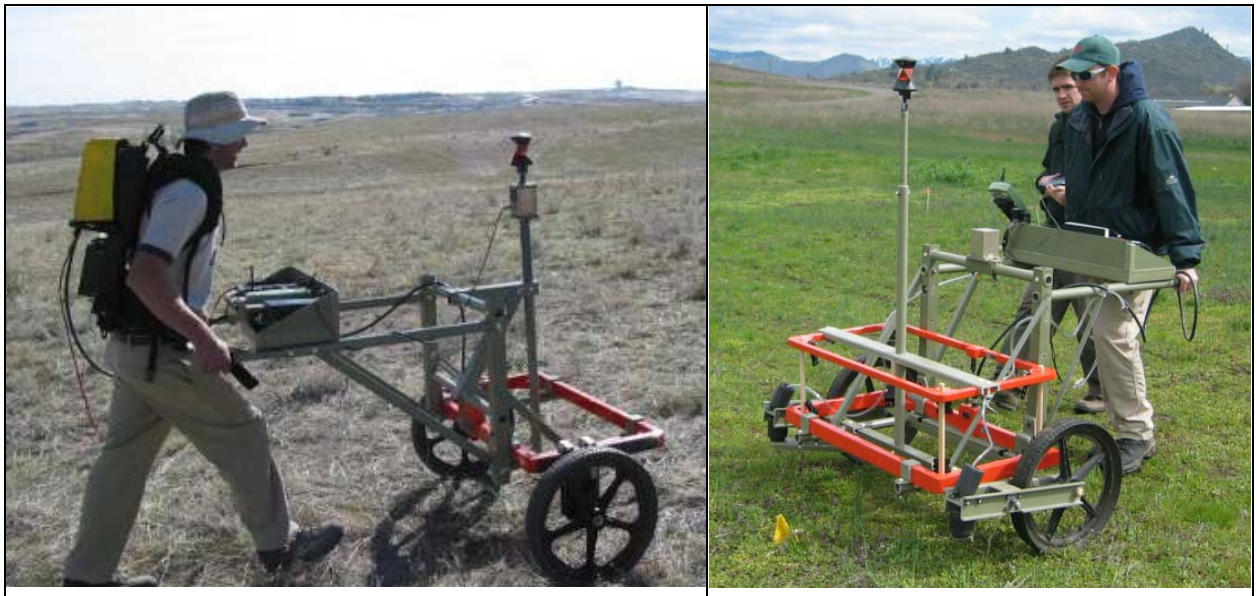

(a) (b)

Figure 13. Modified EM-61 discrimination carts developed as part of this project. (a) First version of the system with Crossbow IMU and RTS. (b) Final version where the coils have been mounted on a suspension cart and the IMU has been moved to a more stable position.

The first modification to the system was tested in 2005 at the FLBGR test-grid. Figure 14 compares that test data with and without using the IMU to correct positions. Close inspection of the uncorrected data reveals several tears in anomalies that look like the chevron patterns that are common when the sensor and positional data streams are not properly synchronized (e.g., the anomaly at 527600 m East, 4384786 m N).

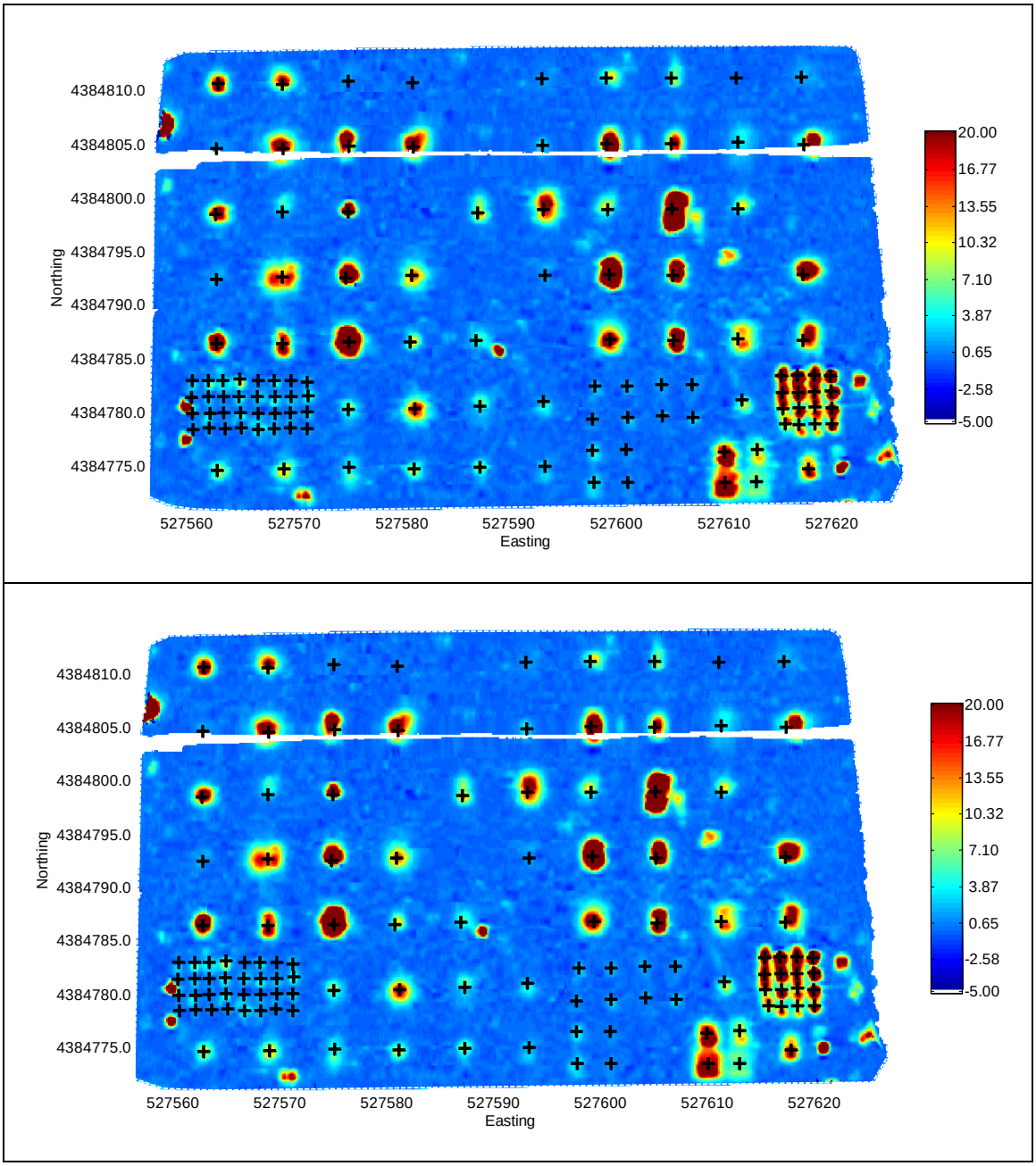

Figure 14. Time channel 3 of EM-61 cart data over the test plot at FLBGR with the locations of buried items shown as black crosses. The top image was made under the assumption that the RTS prism location is vertically above the center of the coil, while in the bottom image the pitch and roll from the Crossbow IMU was used to correct the positions.

However, those same anomalies are not distorted when the pitch and roll from the crossbow are used to correct the location of the RTS prism. Thus, the sensors can be more accurately positioned when including the sensor pitch and roll in the position correction.

After surveying the FLBGR test grid, some additional data were collected on the 20-mm Range Fan and the Rocket Range. During that data collection activity, the output of the Crossbow IMU was found to be unreliable. The Crossbow was undergoing strong accelerations whenever the cart hit a bump due to its position high up on the RTS pole. Therefore, in 2006, the IMU was moved to a position closer to the center of gravity and the system was installed on the suspension cart developed for the EM-63 (see next section). Crossbow data collected with this modified system were more reliable.

The performance of the modified EM-61 (suspension cart, IMU, RTS) was compared to that of a "production standard" EM-61 with a GPS and no IMU. Data collected over the Ashland test plot (see Report 4 for images of the data) were used and three-dipole instantaneous polarization models were fit to each of the single-object cells in the test plot. For the production EM-61 survey, 38 of 45 models had valid fits (data quality good, model and data agree) while for the IMU/RTS survey, 43 of 45 anomalies had valid fits. Good fits to more anomalies indicates that the use of the RTS and the inclusion of the crossbow have improved data quality. Figures 15 through 18 compare various parameters of the extracted polarization tensor models. Both surveys show some spread in the recovered instantaneous amplitudes for each ordnance type, although the IMU/RTS system does appear to be better clustered than the production survey. In most cases, the secondary and tertiary polarizations for UXO items are in relatively close agreement, although there are some exceptions (e.g. the production cart fits to the 37-mm projectile and 60-mm mortar). Comparison of the decay rates reveals that the BLU-28 and M42 have noticeably faster decays than the other items (Figure 16). Predicted decay rates for the other items are relatively consistent, although there is some spread in values, particularly for the secondary polarization. Again, the IMU/RTS parameters tend to cluster together more closely than those from the production survey. Seventy-five percent of locations predicted by the IMU/RTS system lie within 10 cm of the ground-truth location compared to 65 percent for the production system (Figure 17). Depths predicted by the IMU/RTS system are in closer agreement to the true depths (Figure 18).

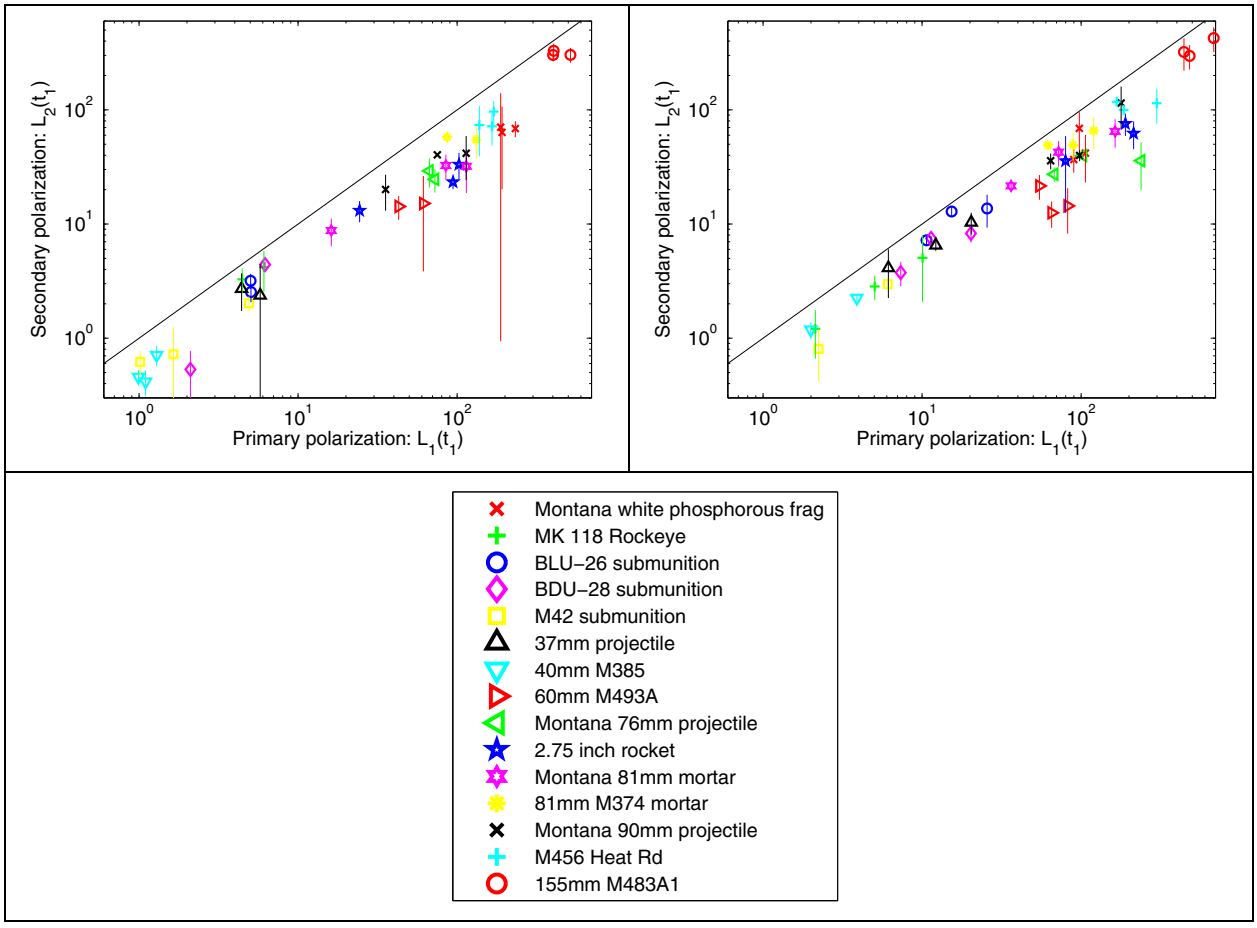

Figure 15. Recovered polarizations at time channel 1 for the EM-61 with GPS and no IMU (on left) and with RTS and IMU (on right). The secondary polarization is plotted as the average of the two smallest polarizations, with a vertical line joining the two values.

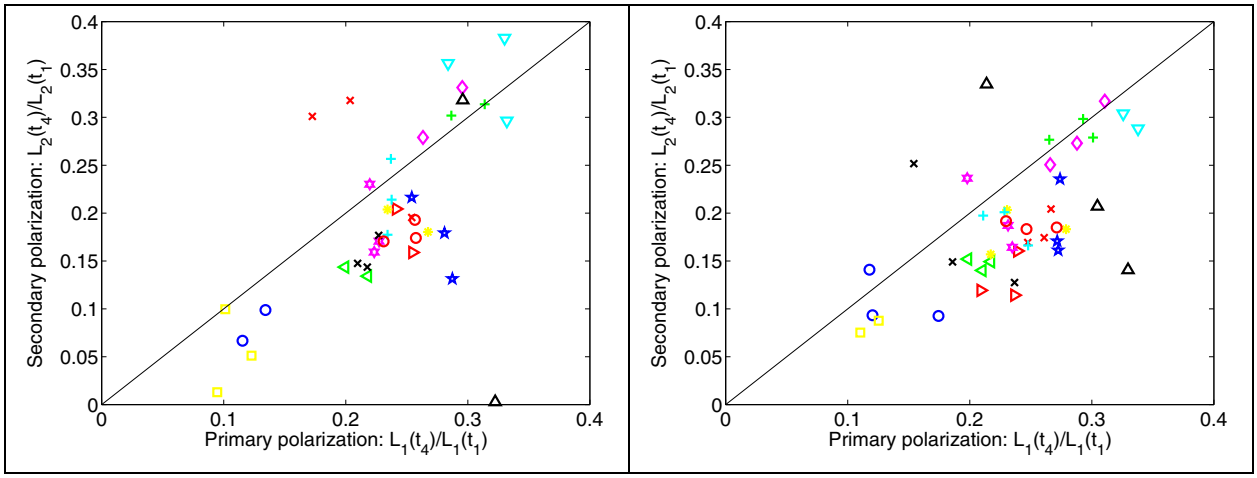

Figure 16. Ratio of recovered polarizations at time channels 1 and 4 for the EM-61 with GPS and no IMU (on left) and with RTS and IMU (on right). Values for both primary and secondary polarizations are shown.

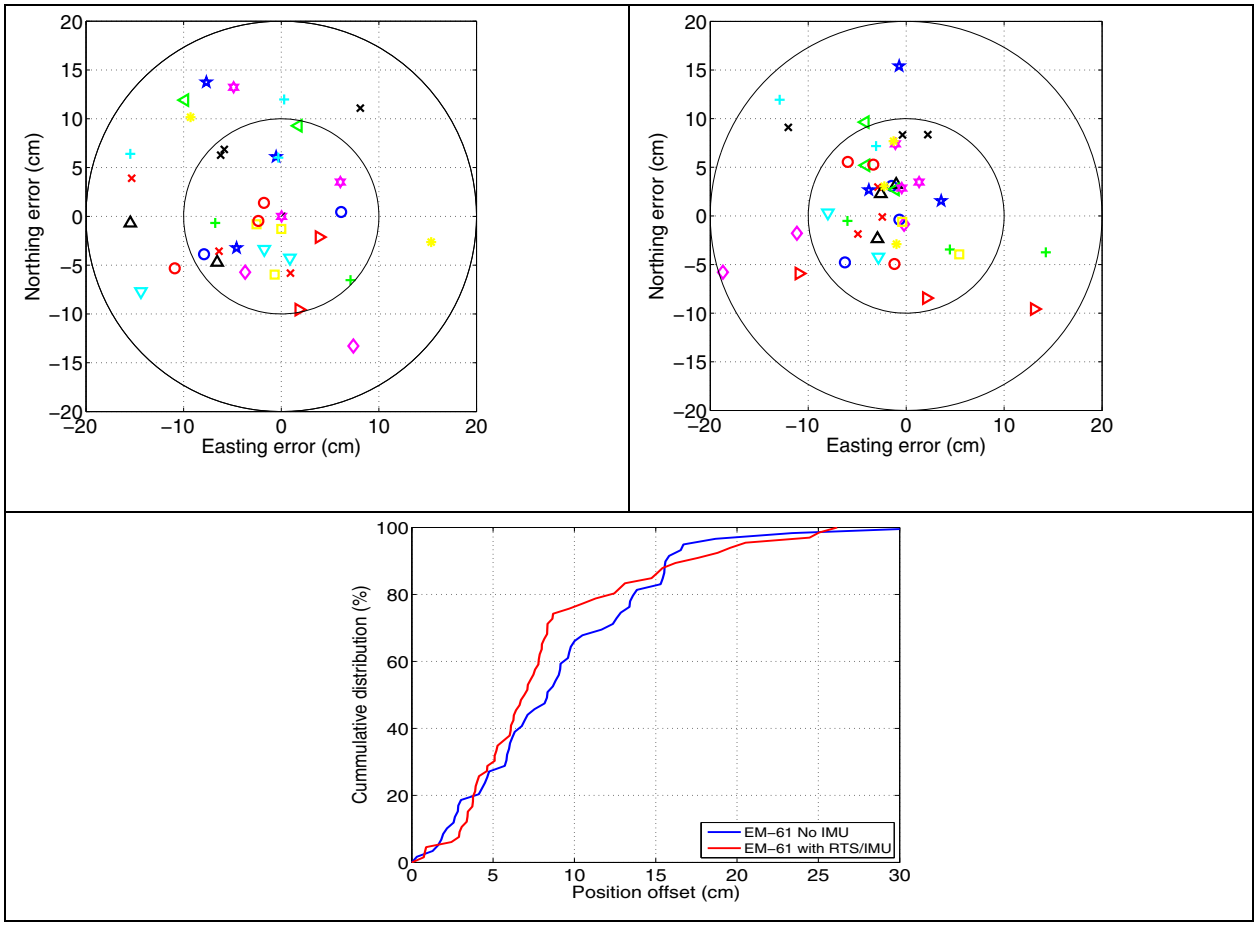

Figure 17. Comparison of the predicted versus ground-truth locations for the EM-61 without IMU (top left) and with IMU and RTS (top right). Circles are drawn at 10 and 20 cm from the true location. A cumulative distribution of the location error reveals that more solutions from the IMU/RTS system are within 10 cm of the correct location.

In conclusion, the modifications to the EM-61 cart have moderately improved the accuracy of the polarization tensor parameters extracted from the data. Potentially useful discrimination attributes include:

- The amplitude of the largest polarization tensor (indicative of size);
- The ratio of the secondary to primary polarizations (indicative of shape);
- The ratio of the secondary to tertiary polarizations (indicative of symmetry);
- The decay rate of the polarization (indicative of size and wall thickness of an object). For the EM-61, this attribute may provide limited information due to the short 1.2-ms time range measured, although thin-walled scrap will likely have time constants short enough to be distinguished.

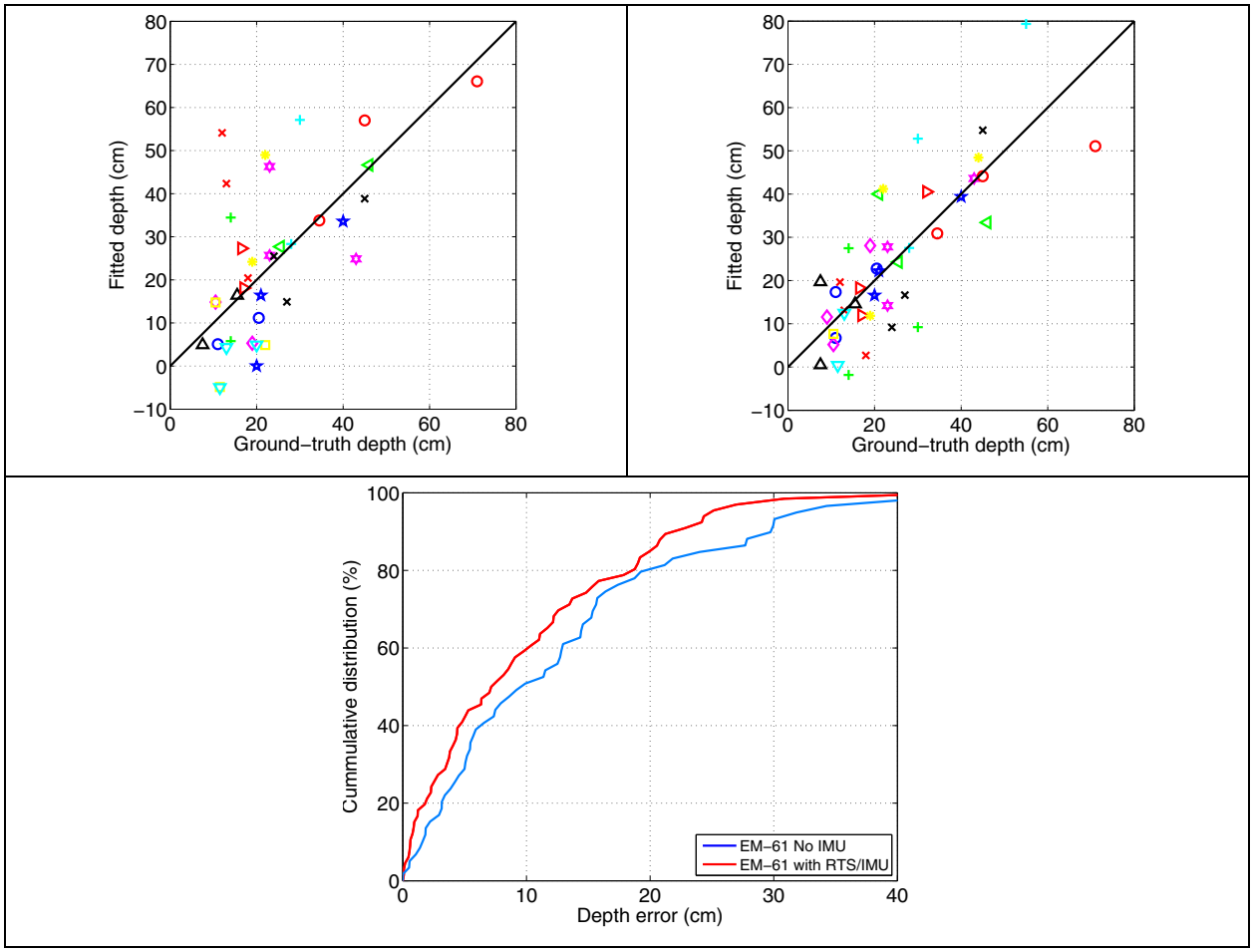

Figure 18. Comparison of the predicted versus ground-truth depths for the EM-61 without IMU (top left) and with IMU and RTS (top right). A cumulative distribution of the depth error reveals that the IMU/RTS system is able to provide a more accurate estimate of depth.

4 EM-63 Cart for Deployment in a Discrimination Mode

Several modifications were made to the EM-63, including the addition of a crossbow IMU for sensor orientation, the use of the robotic total station in place of the GPS, and the development of an air suspension cart that minimizes rapid changes in coil orientation (Figures 19 and 20). The modified cart provides the ability to survey in either discrimination or cued-interrogation mode with the EM63 coil lower to the ground (~30 cm) than the 40 cm for the standard cart. The cart and suspension are shown in the photographs below. The EM63, IMU, and positional data are logged using the Sky Research DAS.

The performance of the modified EM-63 (suspension cart, IMU, RTS) is now compared to that of the standard cart system with a GPS and no IMU. Data collected over the Ashland test plot were used (see Report 4 for more details on the data collection) and three-dipole kbg models were fit to each of the single-object cells in the test plot. The kbg model is a variant of the Pasion-Oldenburg formulation (Pasion and Oldenburg 2001),

$$L_i(t) = k_i \left(t + \alpha_i\right)^{-\beta i} \exp\left(-t / \gamma_i\right) \quad (1)$$

where the early time parameter, $\alpha_i = 0$. There are three polarizations with the convention that $k_1 \geq k_2 \geq k_3$. For a body of revolution, $L_2 = L_3$ for a rod-like object (Pasion and Oldenburg 2001) and $L_1 = L_2$ for a plate-like object.

Figure 19. Modified EM-63 cart, which is lower to the ground and has an air suspension system. The left-hand image provides a close-up of the air-suspension, while the right-hand image shows the cart upside down.

Figure 20. Modified EM-63 cart collecting discrimination mode data at the Ashland test site.

Figures 21 to 25 compare the model parameters recovered by inverting the two different data sets. Careful inspection of the k1 and $(k_2 + k_3)/2$ plot reveals that the parameters are more tightly clustered for the IMU/RTS system (Figure 21). The 20-, 37-, and 155-mm projectiles, and the 60-mm mortars all have distinct parameter values. There are some ordnance types that don't cluster particularly well; these include the 2.75-in. rockets and the 90-mm projectiles. Time-decay parameters (β and γ) recovered from the data also tend to cluster together for each ordnance type (Figure 22), although again there are some outliers (the 90-mm projectile) and the clustering is tighter for the primary compared to the secondary polarizations. Parameters extracted from the Pasion-Oldenburg model, such as the integrated polarization and the relative decay (Figure 23) provide a two-dimensional (2-D) feature space that provides good separation between the different classes. The 37-mm projectiles, in particular, occupy a distinct region of parameter space. There is particularly good separation between the large items (155 mm), the middle-sized items (76 to 105 mm), the small ferrous items (20 mm, Rockeye, BDU-28, and 40 mm) and the small aluminum items (BLU-26 and M42). It would be difficult to further subdivide the ordnance using this feature space; the middle-sized projectiles, in particular, display considerable overlap. Classification using the modified cart with RTS/IMU would be easier and more reliable than for the original cart with GPS only.

The object locations predicted by the modified EM-63 agree more closely with the ground-truth data than the locations predicted by the original system (Figure 24). Approximately 90 percent of the predicted locations from the modified system are within 15 cm of the ground-truth, compared to just over 70 percent for the original system. Predicted depths of the modified system are also better (Figure 25), with 90 percent within 20 cm compared to 75 percent for the original system.

In conclusion, the modifications to the EM-63 cart have significantly improved the accuracy of the polarization tensor parameters extracted from the data. Potentially useful discrimination attributes include:

- The amplitude of the largest polarization tensor, either as k_1, $L_1(t_1)$ or the integral of the polarization (all are indicative of size).
- The ratio of the secondary to primary polarizations (indicative of shape);
- The ratio of the secondary to tertiary polarizations (indicative of symmetry);
- The decay rate of the primary polarization (indicative of size and wall thickness of an object). This can be expressed either with Pasion-Oldenburg β and γ parameters, or the relative decay rate of the polarization (e.g., value at time channel 19 over the value at time channel 1).

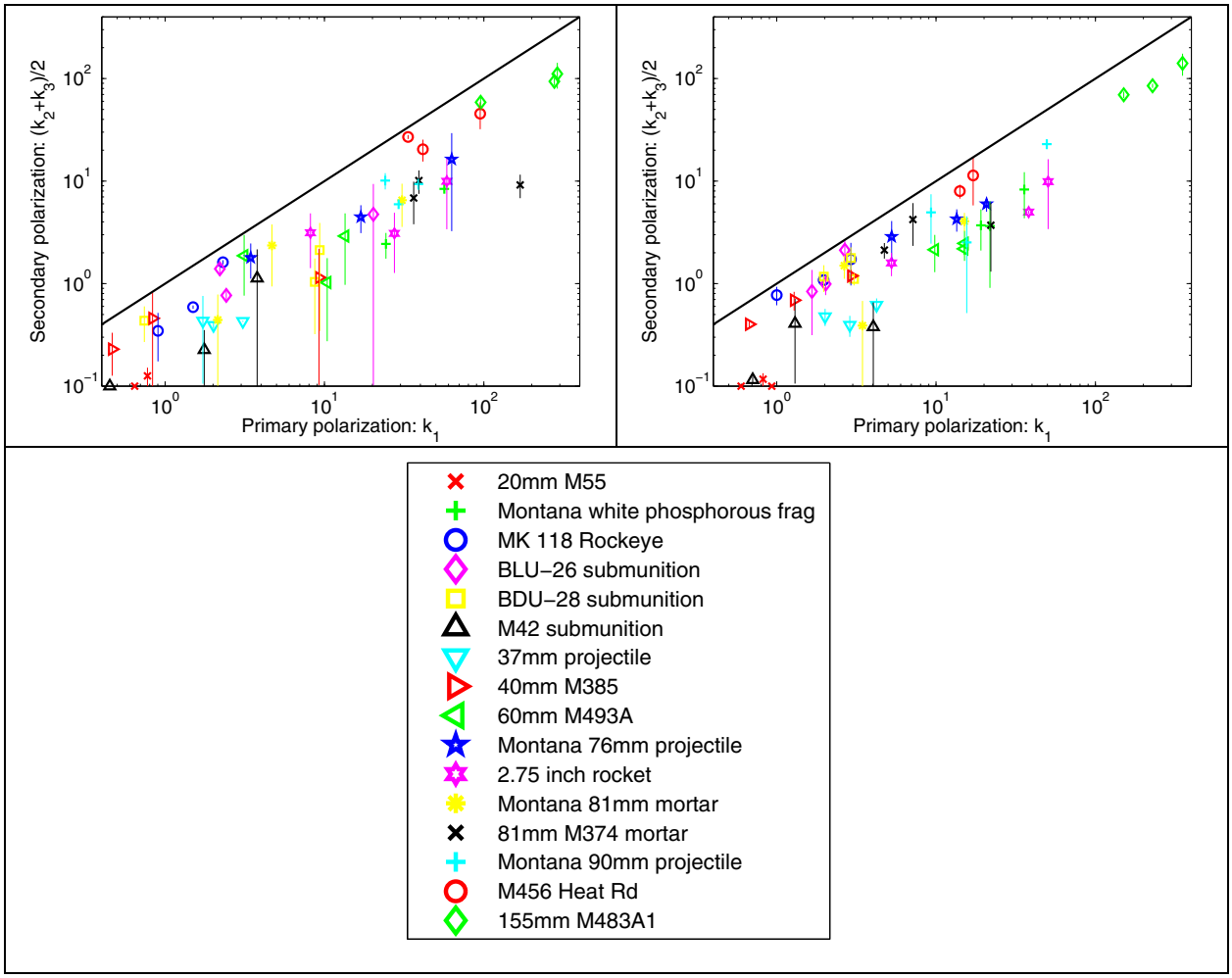

Figure 21. Parameters k_1 and $(k_2 + k_3)/2$ recovered from the EM-63 with GPS and no IMU (on left) and with RTS and IMU (on right). The secondary polarization is plotted as the average of the two smallest polarizations, with a vertical line joining the two values. For an axi-symmetric ferrous object, the two values are equal.

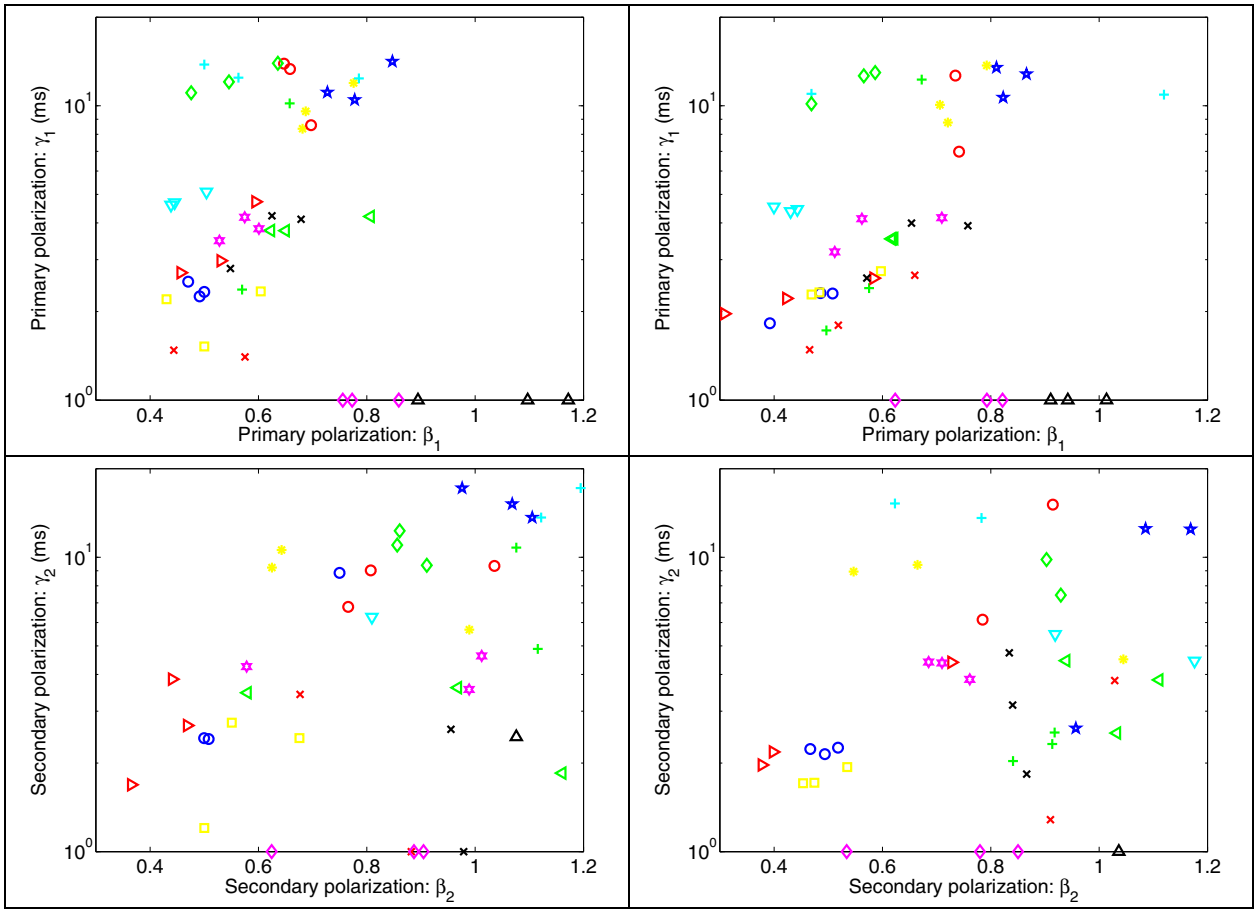

Figure 22. Pasion-Oldenburg β and γ parameters recovered from the EM-63 with GPS and no IMU (on left) and with RTS and IMU (on right). The top row shows values from the primary polarization, the bottom from the secondary polarization.

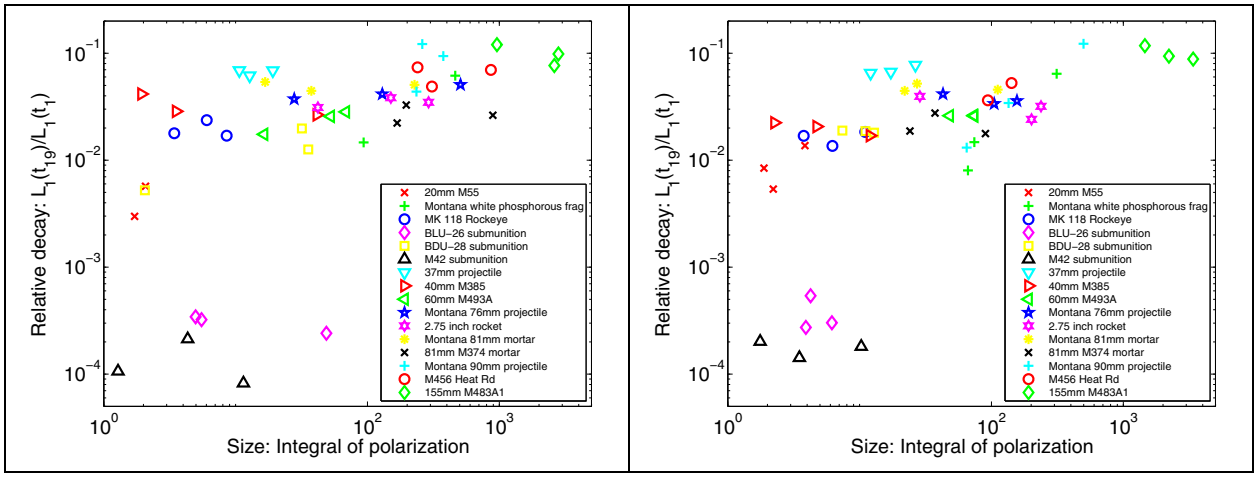

Figure 23. Ratio of the primary polarization at time channels 1 and 19 (180 and 10 ms after pulse turn-off) for the EM-63 with GPS and no IMU (on left) and with RTS and IMU (on right). The bottom axis plots the integral of the polarization.

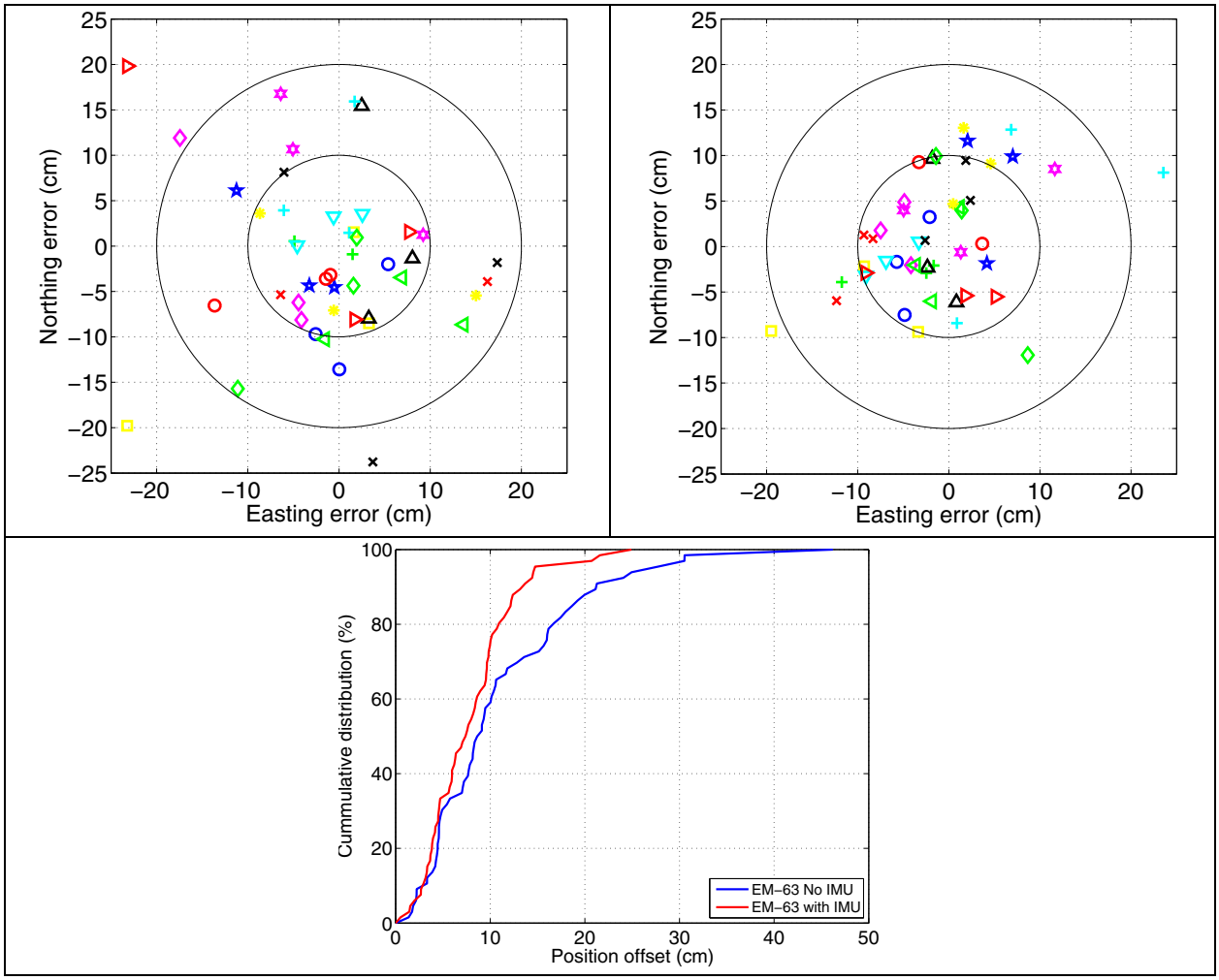

Figure 24. Comparison of the predicted versus ground-truth locations for the EM-63 without IMU (top left) and with IMU and RTS (top right). Circles are drawn at 10 and 20 cm from the true location. A cumulative distribution (bottom left) of the location error reveals that more solutions from the IMU/RTS system are within 10 cm of the correct location.

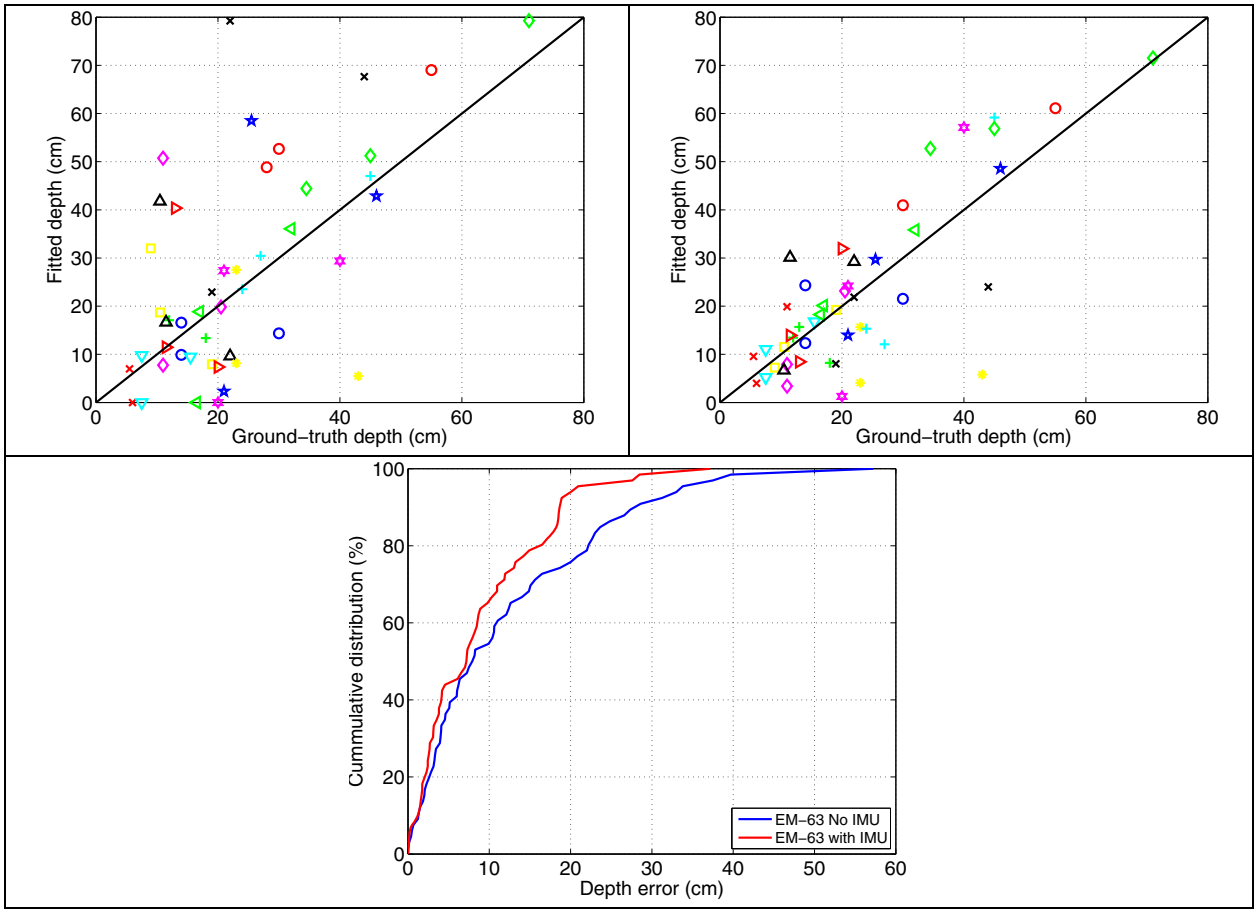

Figure 25. Comparison of the predicted versus ground-truth depths for the EM-61 without IMU (top left) and with IMU and RTS (top right). A cumulative distribution of the depth error reveals that the IMU/RTS system is able to provide a more accurate estimate of depth.

5 Magnetometer Array and Cart for Deployment in a Discrimination Mode

Three different configuration magnetometer systems were developed as part of this project. Each of the systems used the same Geometrics G823 Cesium Vapor total field magnetometers and were positioned with a Leica TPS 1206 RTS augmented by a Crossbow AHRS 400 IMU. By knowing the geometry of each sensor relative to the RTS prism, and the pitch and roll from the IMU, each sensor can be precisely positioned in three dimensions. The three systems were:

1. A man-portable quad-sensor array (Figure 26a) configured with the sensors between 37.5 and 50 cm apart;
2. A cart-based quad-sensor array configured with 0.25-m sensor spacing 0.25 m above the ground (Figure 26b); and
3. A cart-based gradiometer configuration with two lower sensors 0.25 m above the ground at 50-cm spacing and two upper sensors 50 cm directly above the lower sensors (see the schematic in Figure 27).

(a) (b)

Figure 26. Man-portable quad-sensor array (left) and cart-based magnetometer systems developed as part of this project. For the gradient configuration, the same cart was used with the upper sensors 50 cm above the lower ones.

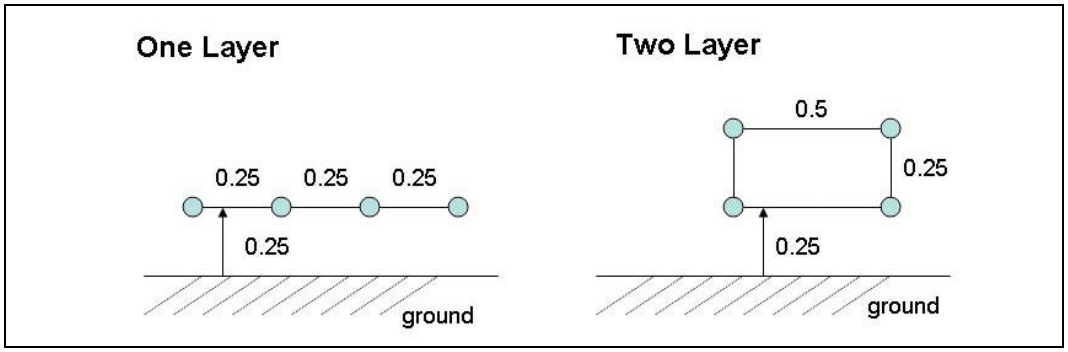

Figure 27. Scenarios for one- and two-layer measurements. All dimensions are listed in meters. The two-layer system used a 0.5-m vertical separation.

Data were collected with each of these systems at the Ashland test plot in May 2006 (see Report 4). This report compares the performance of the magnetometer cart against that of the man-portable magnetometer array without IMU (a system that has been used extensively in Montana to collect production data for the Montana Army National Guard, see Billings and Youmans (2007)). To compare the systems, dipole moments were fit to each of the ferrous single objects in the test plot with caliber greater than 37 mm. Due to variations in the magnetic moment with orientation and potential remanent magnetization, the dipole moment for a given ordnance type may vary widely. Therefore, predicted locations and depths of fitted dipole moments were compared to ground-truth locations and depths (Figures 28 and 29). Locations predicted from the cart data are more accurate, with over 90 percent within 20 cm of the ground-truth position, compared to 90 percent within 30 cm for the man-portable array. Depths are also more accurate with similar performance statistics to locations (that is 90 percent within 20 cm of the correct depth, compared to 90 percent within 30 cm).

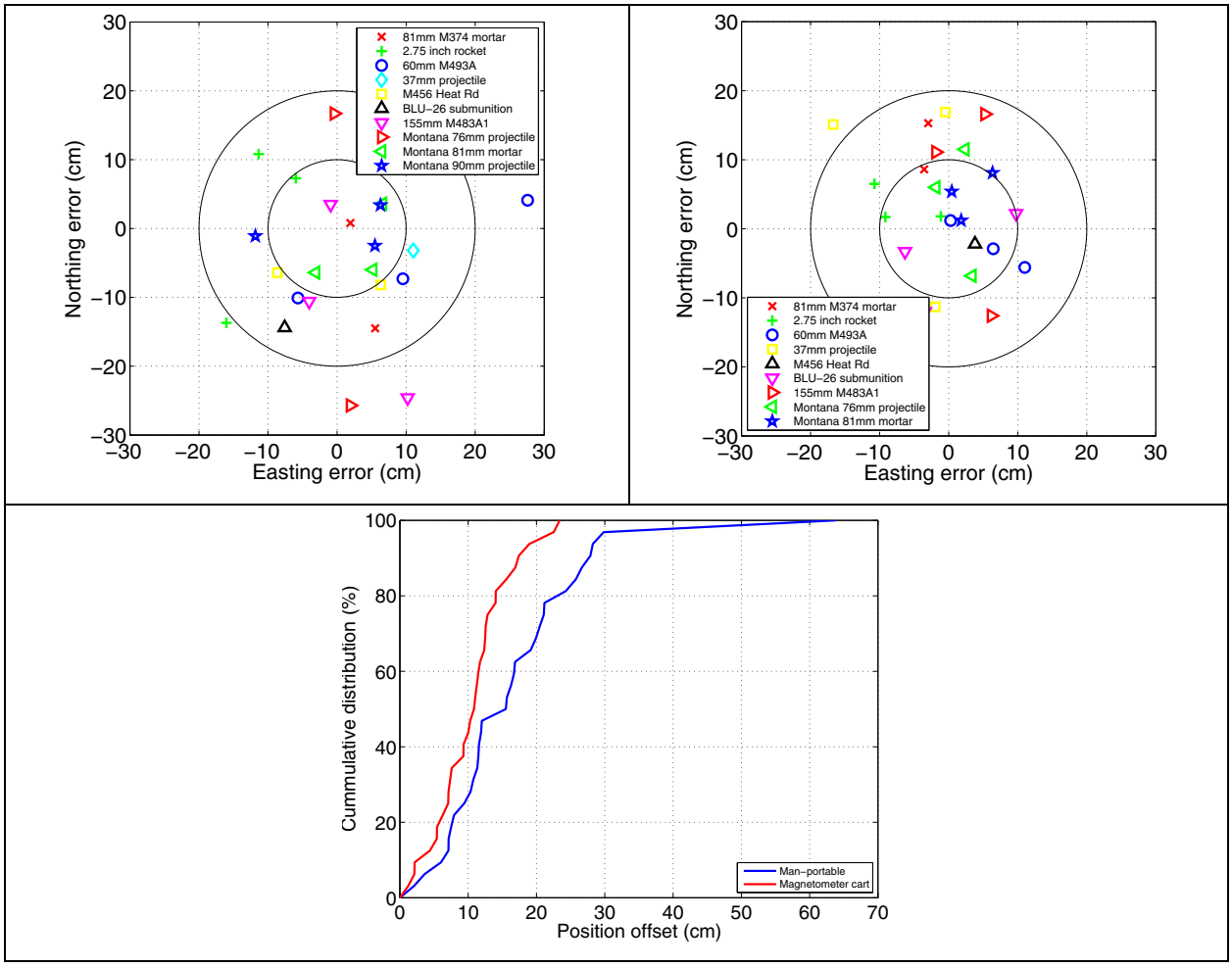

Figure 28. Comparison of the predicted versus ground-truth locations for dipole fits to the man-portable array without IMU (on left) and the magnetometer cart with IMU (on right). A cumulative distribution of the depth error reveals that the IMU/RTS system is able to more accurately estimate depth.

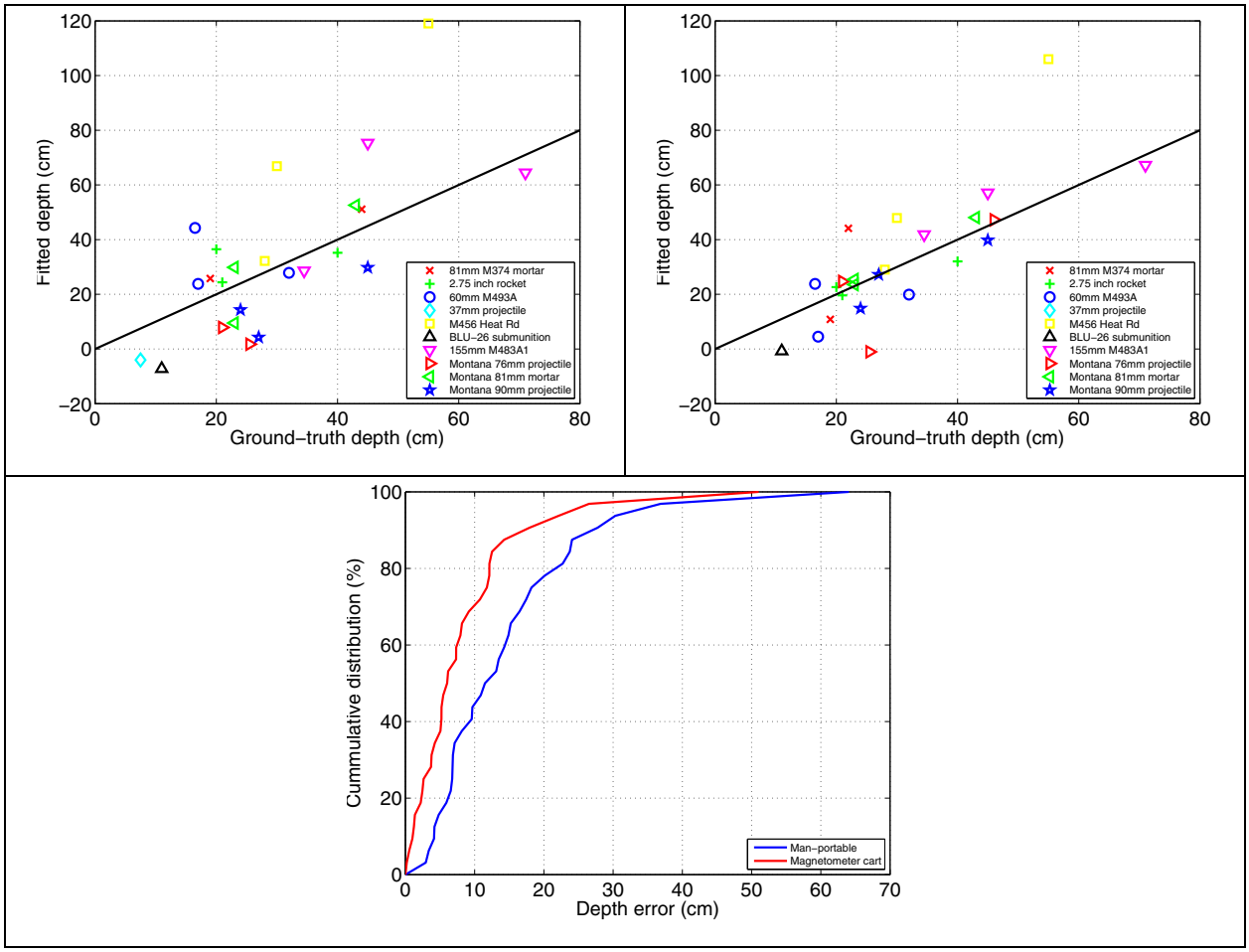

Figure 29. Comparison of the predicted versus ground-truth depths for dipole fits to the man-portable array without IMU (on left) and the magnetometer cart with IMU (on right). A cumulative distribution of the depth error reveals that the IMU/RTS system is able to more accurately estimate depth.

6 EM-63 Cart on Cued-Interrogation Mode

As described in Report 4 on the Ashland test plot, several different strategies for collecting cued-interrogation data with the EM-63 were tested in June 2005. These included methods involving:

1. Static data collection, where the EM-63 is moved to a number of discrete locations and data are collected with the instrument stationary;
2. Dynamic data collection, where the EM-63 collects data while in motion.

Each method has advantages and disadvantages. For the static data collection, positional accuracy and signal-to-noise ratio are maximized but at the expense of lower spatial data density. For dynamic data collection, the spatial sampling coverage is dense, but the positional accuracy and SNR are not as good as for static collection. Analysis of both data sets (Pasion et al. 2007) indicated that it was better to collect the data in dynamic mode due to the greater density of spatial sampling. Thus, the strategy adapted for the rest of the project was to use dynamic data collection over parallel transects spaced 25 cm apart. These lanes were pre-marked on a 2.5-m by 2.5-m tarpaulin (Figure 30) with data generally collected over a 3-m by 3-m square area centered on the estimated anomaly location. To maximize SNR and to minimize high-frequency vibrations, the EM-63 suspension cart and RTS/IMU combination used in the discrimination mode data collection were used again.

Figure 30. Tarpaulin with marked lanes for cued interrogation.

Data colleted over the Ashland test plot during February 2006 were used to compare the performance of the discrimination and cued-interrogation modes (see Report 4). For the discrimination mode data, the same three-dipole Pasion-Oldenburg fits described in Chapter 4 were used. The cued-interrogation data used an equivalent strategy to recover Pasion-Oldenburg models over eight single-object anomalies from the Ashland test plot (two 76-mm, one 90-mm, and three 155-mm projectiles and two 81-mm mortars). The predicted locations appear to be slightly better for the discrimination mode data (Figure 31), although the sample size is quite small so this may not be a significant observation. Both data sets have one model with a 15-cm or greater error in position and six models with an error less than 7.5 cm. Predicted depths for the cued-interrogation data are more accurate (Figure 32), with six of the eight depths within 10 cm of the ground-truth depth compared to three of eight for the discrimination mode data (Figure 32c).

Each of the single objects in the test plot had previously been characterized by dense, spatially accurate, high SNR measurements at the ERDC test stand in Vicksburg (see Report 3). The polarization tensor parameters extracted from the cued-interrogation data are in closer agreement with the test-stand data than those extracted from the discrimination mode data (Figures 33 and 34). The discrimination data fits to one 81-mm mortar and the 90-mm projectile are significantly different from the test-stand fits. In contrast, all k parameters extracted from the cued-interrogation data lie within the range of values found from the test-stand data. In addition, the decay characteristics of the primary polarization are in close agreement (Figure 34).

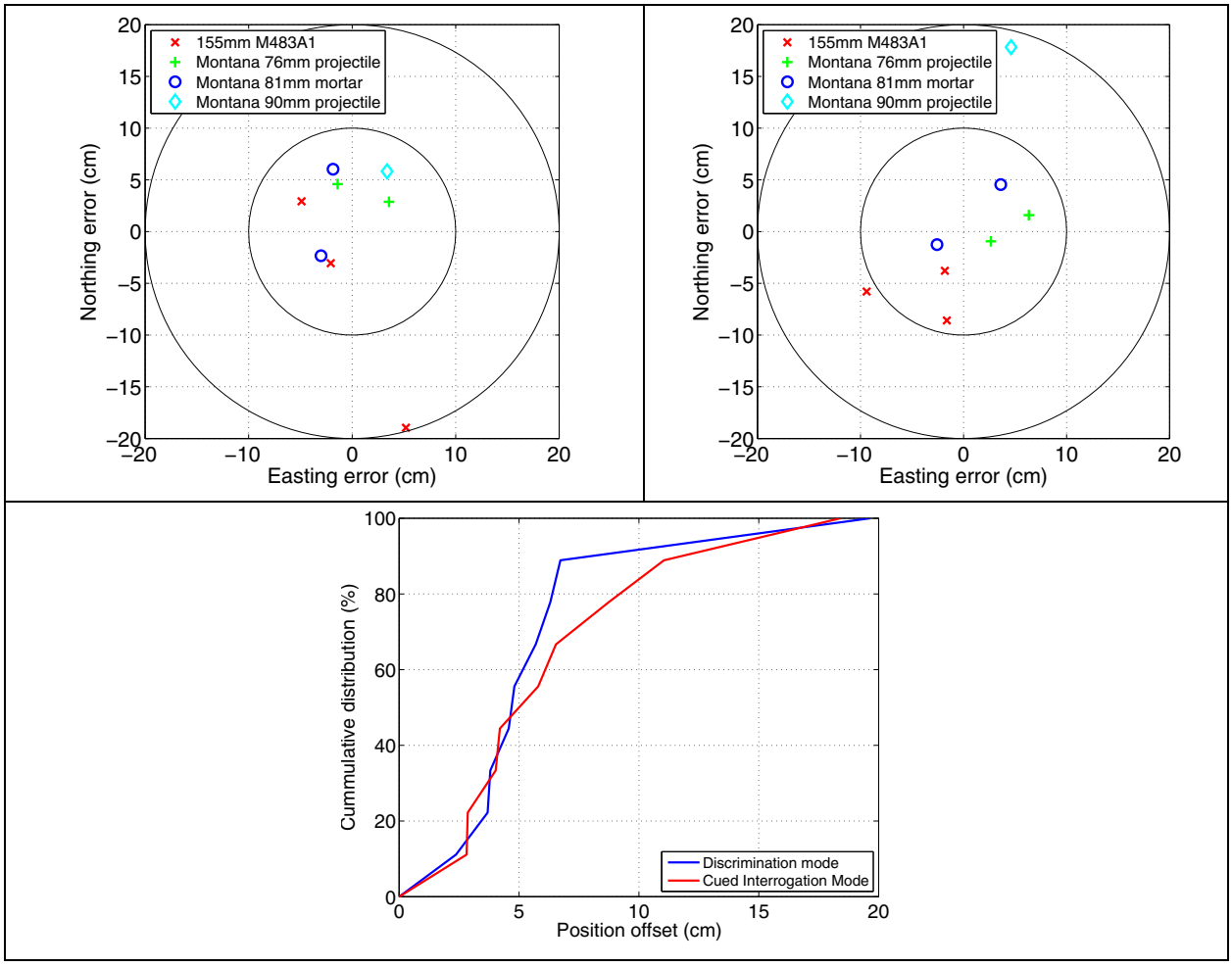

Figure 31. Comparison of the predicted versus ground-truth locations for the EM-63 discrimination (top left) and cued-interrogation data sets (top right). Circles are drawn at 10 and 20 cm from the true location. A cumulative distribution (bottom left) of the location error reveals that locational accuracy of both systems is similar (at least with the small sample size available).

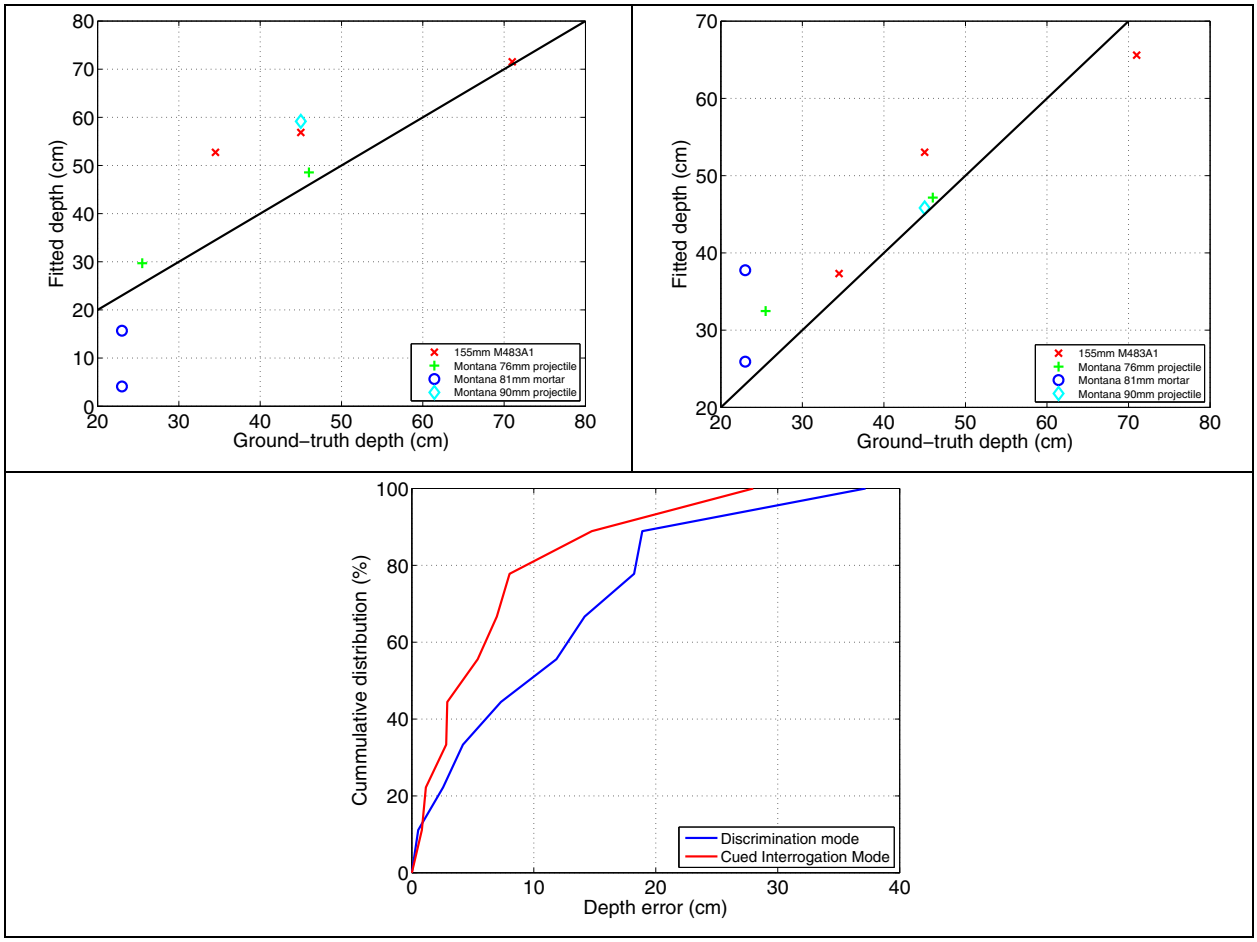

Figure 32. Comparison of the predicted versus ground-truth depths for the EM-63 discrimination (top left) and cued-interrogation data sets (top right). Circles are drawn at 10 and 20 cm from the true location. A cumulative distribution (bottom left) of the depth error reveals that the cued interrogation platform provides more accurate estimates of item depths (at least for the small sample size available).

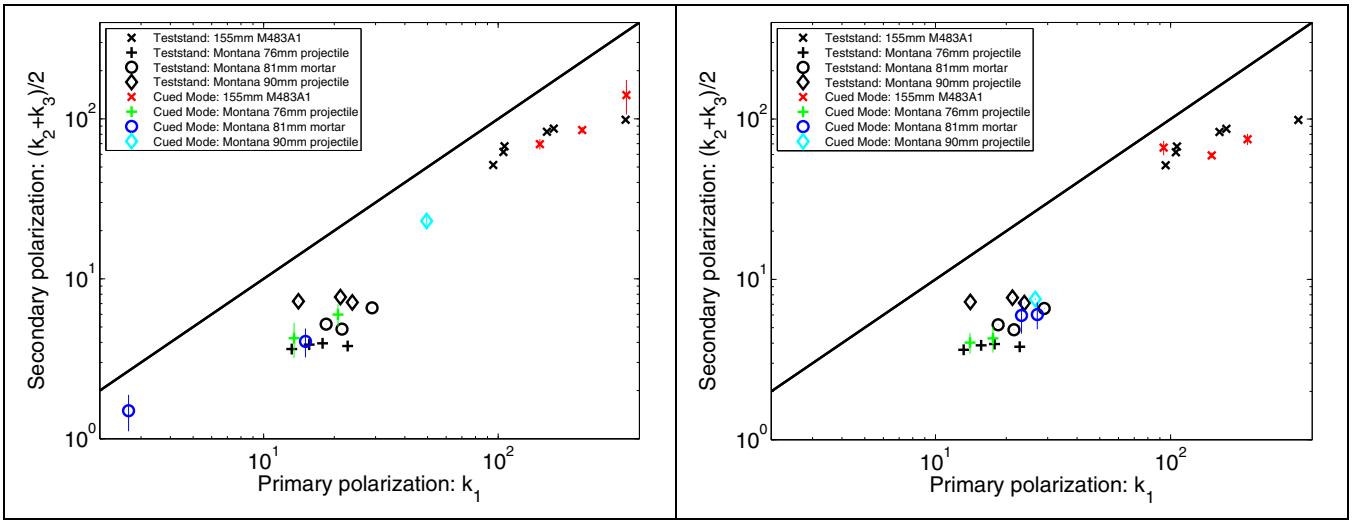

Figure 33. Parameters k_1 and (k_2 + k_3)/2 recovered from the EM-63 deployed in discrimination (on left) and cued-interrogation (on right) modes. Also shown in black are the values for the same items measured on the test stand at Vicksburg. The secondary polarization is plotted as the average of the two smallest polarizations, with a vertical line joining the two values. For an axi-symmetric ferrous object, the two values are equal.

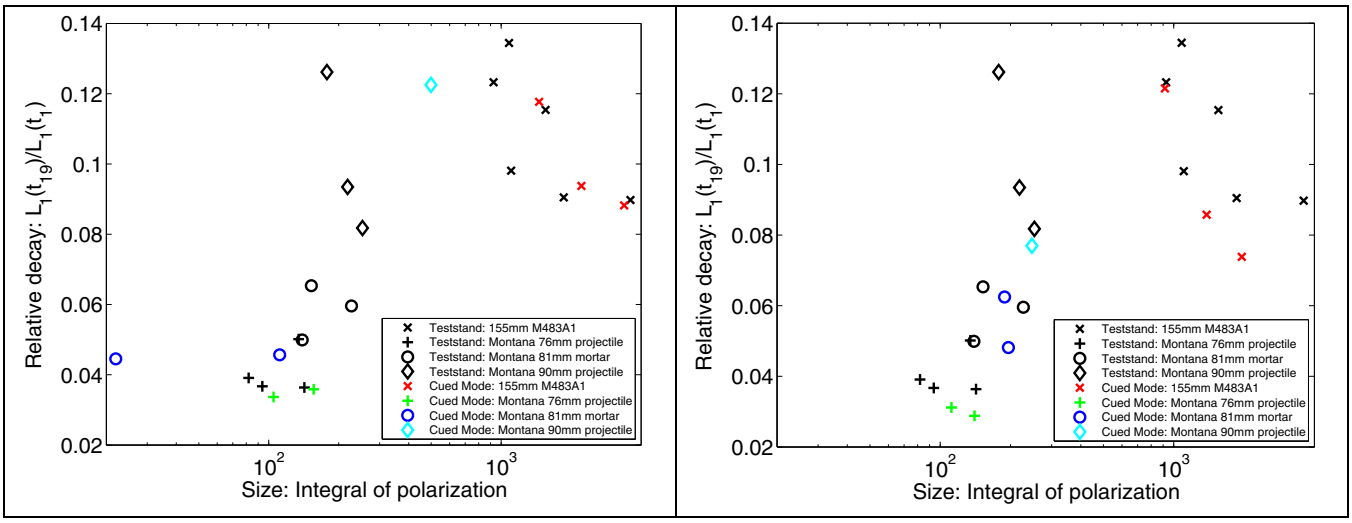

Figure 34. Ratio of the primary polarization at time channels 1 and 19 (180 and 10 ms after pulse turn-off) for the EM-63 deployed in discrimination (on left) and cued-interrogation (on right) modes. The bottom axis plots the integral of the polarization. Also shown in black are the values for the same items measured on the test stand at Vicksburg.

7 Cued Interrogation with the GEM-3

Measurements in 2005 with the Geophex GEM-3 with the 40-m head demonstrated that the instrument had good performance against small objects. The GEM-3 was used for cued interrogation of small objects such as 37-mm projectiles. After testing a number of methods for data collection, a 1-m × 1-m template consisting of 49 measurement locations was selected. A schematic of the template is shown in Figure 35. Approximately five seconds of data were collected at each location on the template (Figure 36a). At the 50th survey location, a fiberglass jig was used to collect data at a second elevation (3 cm higher) in the center of the template (Figure 36b).

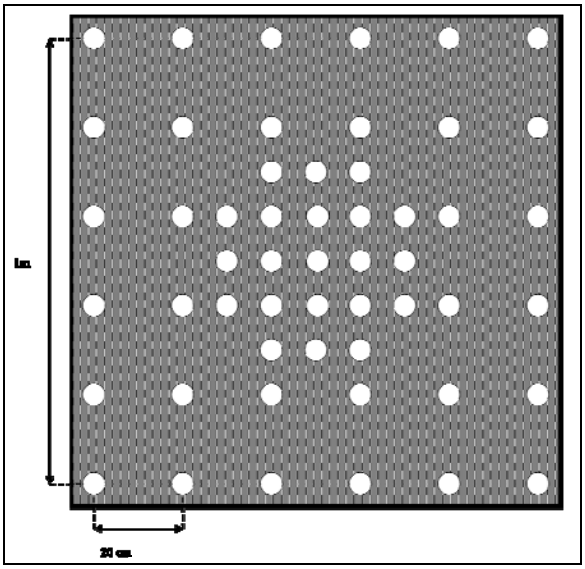

Figure 35. Schematic of the template used for GEM surveying. The 36 holes in the main grid are separated by 20 cm. The center of the template contains 17 extra holes to increase the density to 10 cm directly over the target. The four corners of the template were not surveyed. This resulted in 49 survey locations.

The template was moved four times to cover a 2- × 2-m area and measure larger, deeper anomalies. Each of the 1- × 1-m areas was measured with a uniform grid of 36 points with 20-cm station separation. Each of the four segments represented a quadrant of the final survey area as shown by the schematic in Figure 37. To ensure complete coverage, the edges of the four surveys overlap.

Performance of the GEM-3 and the cued-interrogation procedure is assessed in Report 9 on the FLGBR.

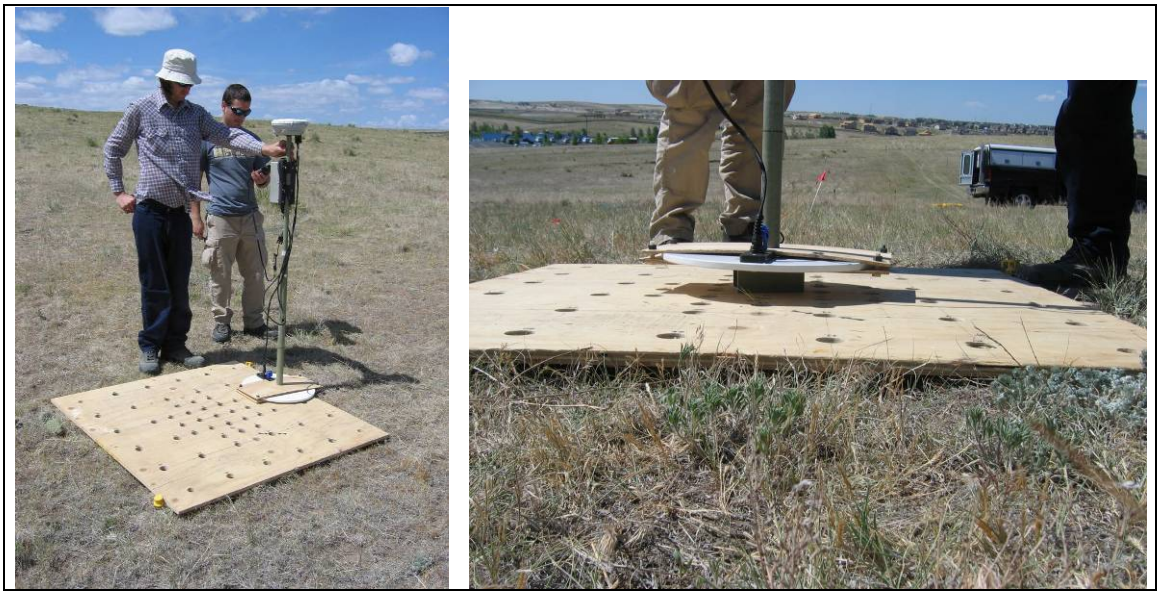

Figure 36. Template used for GEM-3 Cued Interrogation data collection. Photo on right is a fiberglass jig used to collect data at a second elevation (3 cm above template) at the center of the template.

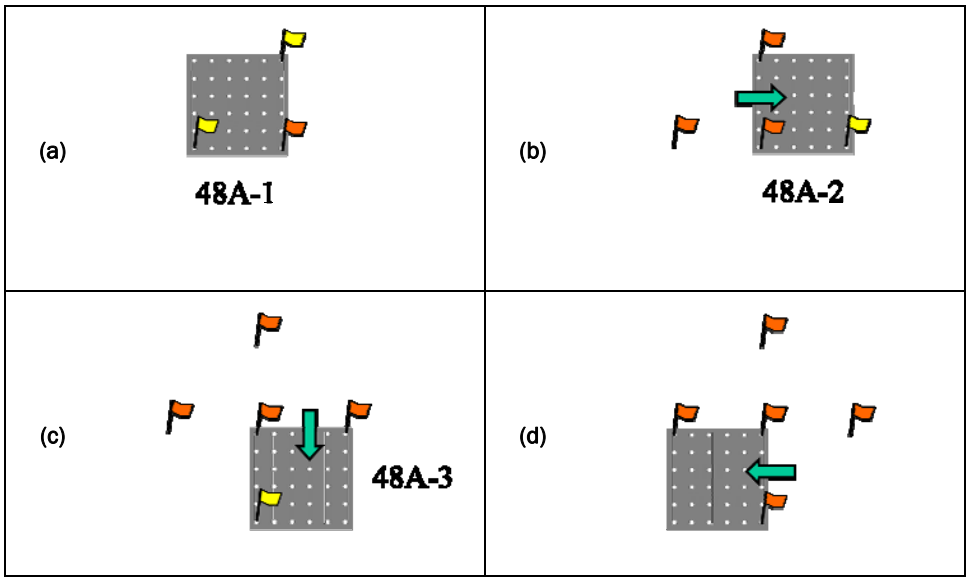

Figure 37. Schematic of the survey procedure for large targets and multi-object cells using a 1- x 1-m template. In each panel the orange pin flags represent flags that have been placed in the ground to locate the template. The yellow pin flags represent new flags that are placed in the ground and will be used during subsequent surveys. The green arrows indicate the direction the template has been moved.

8 Conclusions

A significant component of the work conducted under this contract involved the modification and development of discrimination and cued-interrogation platforms and procedures. For primary positioning, each of the systems used the Leica TPS-1206 RTS in place of a GPS and a Crossbow AHRS 400 IMU for sensor orientation information and to further refine the RTS positions. Performance of the modified systems was superior to a pre-existing baseline system:

1. Discrimination and detection mode, Geonics EM-61 five-element towed array with RTS/IMU: Including the IMU substantially improved positional accuracy (90 percent of IMU-aided locations within 8 cm of the measured location compared to 90 percent within 23 cm for the unaided system). This system was deployed to the FLBGR and Camp Lejeune sites (see Reports 8 and 9 for details);
2. Discrimination mode, Geonics EM-61 on suspension cart with IMU/RTS. The Ashland test plot was used to compare the performance of the new system against a production standard EM-61 positioned with GPS. Three-dipole instantaneous polarization fits to the new system had more accurate locations and depths (compared to ground-truth) than the production standard EM-61. In addition, polarization parameters for each class of ordnance were more tightly clustered, indicating that the new system has superior discrimination ability;
3. Discrimination mode, Geonics EM-63 suspension cart with IMU/RTS. The Ashland test plot was used to compare the performance of the new system against an EM-63 positioned with GPS alone. Three-dipole Pasion-Oldenburg fits to the new system had more accurate locations and depths than the EM-63 with GPS. In addition, polarization parameters for each class of ordnance were more tightly clustered, indicating that the new system has superior discrimination ability. This system was deployed to the FLBGR and Camp Lejeune sites (see Reports 8 and 9 for details);
4. Discrimination mode, Geometrics G823 magnetometer cart with IMU/RTS. Dipole moment depths and locations predicted from the cart data are more accurate than those predicted from a production man-portable magnetometer array (90 percent of locations and depths within 20 cm for the cart, compared to 90 percent within 30 cm for the production man-portable array);

5. Cued-interrogation mode, Geonics EM-63 suspension cart with IMU/RTS and “magic-carpet.” Preliminary tests indicated that a dynamic mode of data collection would provide more accurate feature vectors than a static data collection mode (for the same amount of time spent collecting data). Models extracted from the cued-interrogation data predict more accurate depths and locations than those extracted from discrimination mode data. In addition, the resulting feature vectors are in closer agreement with models extracted from high-quality test stand data. This system was deployed to the FLBGR Rocket Range site (see Report 9 for details).

References

Billings, S. D., and C. Youmans. 2007. Experiences with unexploded ordnance discrimination at a live-site in Montana. *Journal of Applied Geophysics* 61(3-4):194–205.

Pasion, L., and D. Oldenburg. 2001. A discrimination algorithm for UXO using time domain electromagnetics. *Journal of Engineering and Environmental Geophysics* 28(2):91–102.

Pasion, L. P., S. D. Billings, D. W. Oldenburg, and S. E. Walker. 2007. Application of a library based method to time domain electromagnetic data for the identification of unexploded ordnance. *Journal of Applied Geophysics* 61(3-4): 279–291.

REPORT DOCUMENTATION PAGE

Form Approved
OMB No. 0704-0188

1. REPORT DATE *(DD-MM-YYYY)*	2. REPORT TYPE	3. DATES COVERED *(From - To)*
September 2008	Report 5 of 9	

4. TITLE AND SUBTITLE

UXO Characterization: Comparing Cued Surveying to Standard Detection and Discrimination Approaches: Report 5 of 9 – Optimized Data Collection Platforms and Deployment Modes for Unexploded Ordnance Characterization

5a. CONTRACT NUMBER
W912HZ-04-C-0039

5b. GRANT NUMBER

5c. PROGRAM ELEMENT NUMBER

6. AUTHOR(S)

Stephen D. Billings, Leonard R. Pasion, Kevin Kingdon, Sean Walker, and Jon Jacobson

5d. PROJECT NUMBER

5e. TASK NUMBER

5f. WORK UNIT NUMBER

7. PERFORMING ORGANIZATION NAME(S) AND ADDRESS(ES)

Sky Research, Inc.
445 Dead Indian Memorial Road
Ashland, OR 97520

8. PERFORMING ORGANIZATION REPORT NUMBER

ERDC/EL TR-08-36

9. SPONSORING / MONITORING AGENCY NAME(S) AND ADDRESS(ES)

Headquarters, U.S. Army Corps of Engineers
Washington, DC 20314-1000;
U.S. Army Engineer Research and Development Center
Environmental Laboratory
3909 Halls Ferry Road, Vicksburg, MS 39180-6199

10. SPONSOR/MONITOR'S ACRONYM(S)

11. SPONSOR/MONITOR'S REPORT NUMBER(S)

12. DISTRIBUTION / AVAILABILITY STATEMENT

Approved for public release; distribution is unlimited.

13. SUPPLEMENTARY NOTES

14. ABSTRACT

Discrimination and cued-interrogation platforms and procedures developed under contract W912HZ-04-C-0039 are described. Discrimination platform development included: (1) Upgrading Sky's (Sky Research, Inc.) existing EM61 towed array to use five sensors and the Crossbow Inertial Measurement Unit (IMU) for orientation. The IMU significantly improved the positional accuracy of the system. (2) Upgrading a Geonics EM-61 cart-based sensor system to incorporate Robotic Total Station (RTS) positioning, an IMU, and a suspension cart. Compared to a production standard EM-61 positioned with GPS, polarization tensor fits were more accurately positioned and parameter classes more tightly clustered. (3) Upgrading the Geonics EM-63 with RTS, IMU, and a suspension system. Polarization tensor fits were more accurately positioned and parameter classes were more tightly clustered than an equivalent production system. 4) Upgrading a Geometrics G823 magnetometer man-portable quad-sensor array and cart, to include RTS and IMU. Dipole moment depths and locations were more accurate than those predicted from a production level man-portable magnetometer array. Cued-interrogation platforms/procedures development included (1) EM-63 with RTS/IMU/suspension cart and a "magic carpet." Polarization tensor fits to the cued interrogation agreed closely with parameters derived from test stands. (2) GEM-3, 40-cm sensor head and a plywood template. Performance of that system is assessed in Report 9.

15. SUBJECT TERMS

EMI sensors
Frequency-domain electromagnetic induction (FEM)
Ground penetrating radar
Time-domain electromagnetic induction (TEM)
Total-field magnetics
Unexploded ordnance (UXO)
UXO discrimination

16. SECURITY CLASSIFICATION OF:			17. LIMITATION OF ABSTRACT	18. NUMBER OF PAGES	19a. NAME OF RESPONSIBLE PERSON
a. REPORT	b. ABSTRACT	c. THIS PAGE			19b. TELEPHONE NUMBER *(include area code)*
UNCLASSIFIED	UNCLASSIFIED	UNCLASSIFIED		54	